JACS
JOURNAL OF THE AMERICAN CHEMICAL SOCIETY
Article
pubs.acs.org/JACS

Dissymmetric Bis(dipyrrinato)zinc(II) Complexes: Rich Variety and Bright Red to Near-Infrared Luminescence with a Large Pseudo-Stokes Shift

Ryota Sakamoto,*[,†,‡] Toshiki Iwashima,[†] Julius F. Kögel,[†] Shinpei Kusaka,[†] Mizuho Tsuchiya,[†] Yasutaka Kitagawa,[§] and Hiroshi Nishihara*[,†]

[†]Department of Chemistry, Graduate School of Science, The University of Tokyo, 7-3-1, Hongo, Bunkyo-ku, Tokyo 113-0033, Japan
[‡]JST-PRESTO, 4-1-8, Honcho, Kawaguchi, Saitama 332-0012, Japan
[§]Division of Chemical Engineering, Department of Materials Engineering Science, Graduate School of Engineering Science, Osaka University, 1-3, Machikaneyama, Toyonaka, Osaka 560-8531, Japan

Supporting Information

ABSTRACT: Bis(dipyrrinato)metal(II) and tris(dipyrrinato)-metal(III) complexes have been regarded as much less useful luminophores than their boron difluoride counterparts (4,4-difluoro-4-bora-3a,4a-diaza-*s*-indacenes, BODIPYs), especially in polar solvent. We proposed previously that dissymmetry in such metal complexes (i.e., two different dipyrrinato ligands in one molecule) improves their fluorescence quantum efficiencies. In this work, we demonstrate the universality and utility of our methodology by synthesizing eight new dissymmetric bis(dipyrrinato)zinc(II) complexes and comparing them with corresponding symmetric complexes. Single-crystal X-ray diffraction analysis, ^{1}H and ^{13}C NMR spectroscopy, and high-resolution mass spectrometry confirm the retention of dissymmetry in both solution and solid states. The dissymmetric complexes all show greater photoluminescence (PL) quantum yields (ϕ_{PL}) than the corresponding symmetric complexes, allowing red to near-infrared emissions with large pseudo-Stokes shifts. The best performance achieves a maximum PL wavelength of 671 nm, a pseudo-Stokes shift of 5400 cm^{-1}, and ϕ_{PL} of 0.62−0.72 in toluene (dielectric constant ε_s = 2.4), dichloromethane (ε_s = 9.1), acetone (ε_s = 21.4), and ethanol (ε_s = 24.3). The large pseudo-Stokes shift is distinctive considering BODIPYs with small Stokes shifts (~500 cm^{-1}), and the ϕ_{PL} values are higher than or comparable to those of BODIPYs fluorescing at similar wavelengths. Electrochemistry and density functional theory calculations illustrate that frontier orbital ordering in the dissymmetric complexes meets the condition for efficient PL proposed in our theory.

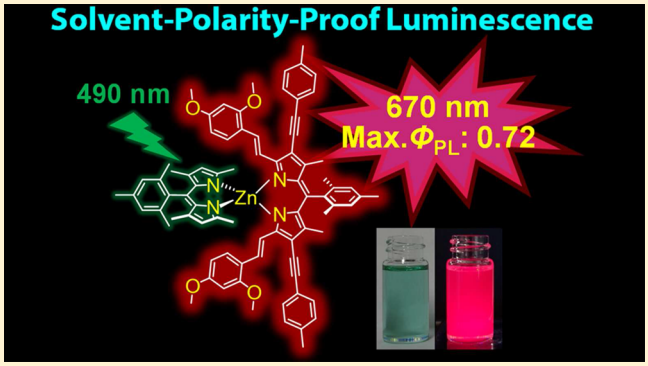

INTRODUCTION

Dipyrrin is a planar molecule consisting of two pyrrole rings bridged by a methine group. Its π-conjugation allows dipyrrin to absorb visible light efficiently through the $^{1}\pi-\pi^{*}$ transition. The dipyrrinato ligand is a monovalent bidentate ligand that forms upon the deprotonation of dipyrrin and can coordinate to various cationic species. The most common dipyrrin complex is 4,4-difluoro-4-bora-3a,4a-diaza-*s*-indacene (BODIPY), which exhibits intense fluorescence, typically at 500−520 nm with a small Stoke shift (~500 cm^{-1}).[1] The flexible modifiability of dipyrrin means that the fluorescence wavelength of BODIPYs can be tuned. These features make BODIPYs suitable for applications such as luminescent bioprobes[2] and laser dyes.[3]

Dipyrrin−metal complexes have been reported as convenient components for supramolecules,[4,5] coordination polymers,[4,6] and metal−organic frameworks[4,7] due to the spontaneous coordination between the dipyrrin ligands and the metal ions. However, little attention has been paid to their photochemistry and photophysics. They have been considered negligible or weak luminophores, although several efforts have been made to improve their luminescence.[8] Lindsey, Bocian, and Holten found that the fluorescence quantum yield of bis(dipyrrinato)-zinc(II) complexes was improved by introducing bulky aryl groups at the meso position,[9] although emission quenching upon symmetry-breaking charge separation in polar solvents was still significant.[10] Cheprakov reported strong fluorescence in mono(dipyrrinato)zinc(II) and calcium(II) complexes supported by ancillary ligands such as acetate and acetylacetonate,[11] although the complexes disproportionated into the corresponding non-fluorescent symmetric complexes or hydrolyzed. Under the background, in previous work we demonstrated another strategy to improve the luminescence of

Received: February 25, 2016
Published: April 4, 2016

DOI: 10.1021/jacs.6b02128
J. Am. Chem. Soc. 2016, 138, 5666−5677

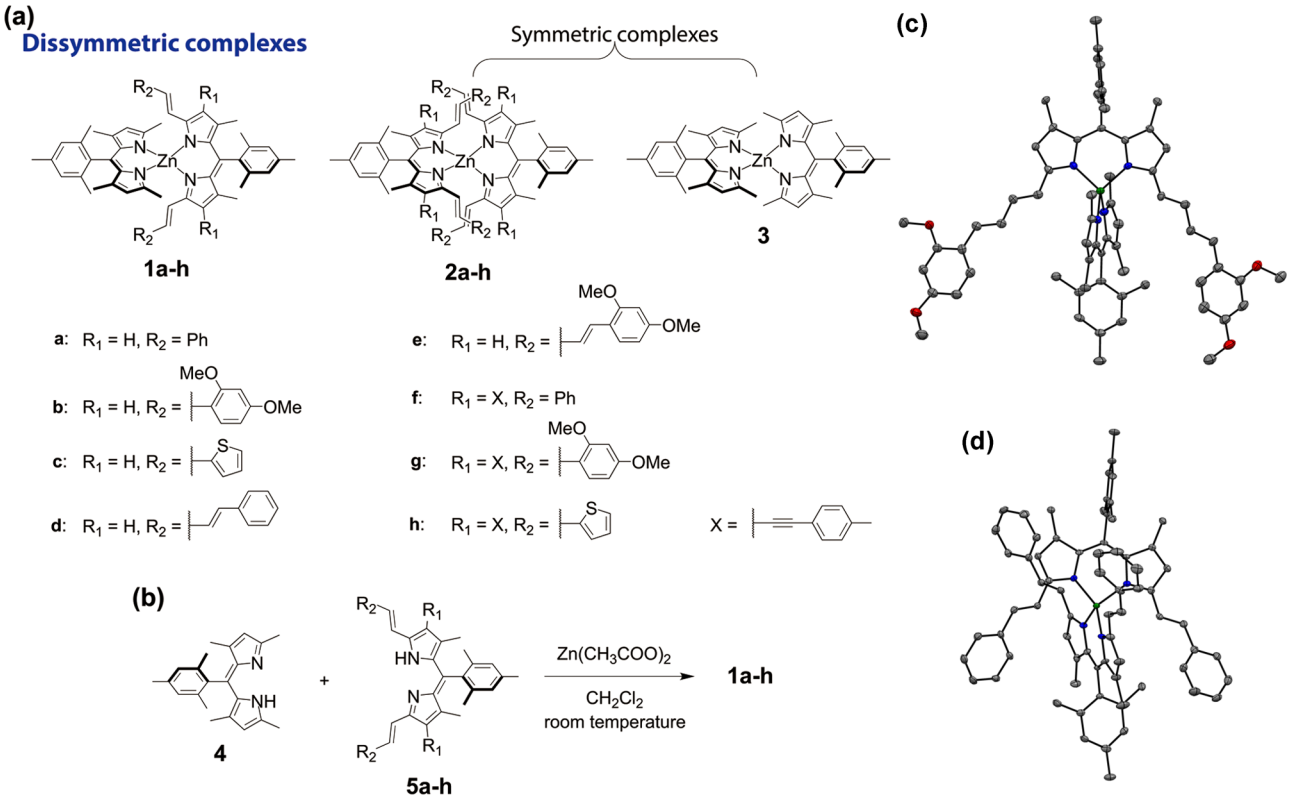

Figure 1. (a) Structures of dissymmetric complexes **1a–h** and symmetric reference complexes **2a–h** and **3**. (b) Synthetic scheme for dissymmetric complexes **1a–h**. ORTEP drawings of (c) dissymmetric **1e·CH_2Cl_2** and (d) symmetric **2a·CH_3OH** with a thermal ellipsoids set at the 50% probability level. Gray, carbon; red, oxygen; blue, nitrogen; green, zinc. Hydrogen atoms and crystal solvent molecules are omitted for clarity.

dipyrrinato–metal complexes. A dissymmetric bis(dipyrrinato)-zinc(II) complex with two different dipyrrinato ligands showed a higher fluorescence quantum yield than the corresponding symmetric complexes (Figure S1, Supporting Information).[12a] The dissymmetric complex retained its bright luminescence even in polar solvents, and was robust enough to resist disproportionation in the solution phase. Dissymmetric bis and tris(dipyrrinato)metal complexes were previously synthesized by Cohen,[13a] Radecka,[13b,c] and Dolphin,[13d] although they did not examine the photophysics of the complexes. We also reported that the introduction of dissymmetry also enhanced the luminescence of tris(dipyrrinato)indium(III) complexes (Figure S2).[12b]

This paper reports eight new dissymmetric bis(dipyrrinato)-zinc(II) complexes (**1a–h**, Figure 1a), focusing on the following areas: (1) justifying our strategy for enhancing the luminescence of dipyrrin–metal complexes; (2) demonstrating the rich variety of dissymmetric complexes; (3) obtaining bright luminescence with tunable wavelengths, especially focusing on red and near-infrared (NIR) emissions; and (4) realizing large pseudo-Stokes shifts.[14] Corresponding symmetric complexes **2a–h** and **3** (Figure 1a) are also studied as references. In addition to photophysical measurements, such as UV/vis, photoluminescence (PL), and PL lifetime measurements, single-crystal X-ray structure analysis, electrochemistry, and density functional theory (DFT) calculations were used to explore the four areas of interest.

RESULTS

Design and Synthesis of Dissymmetric Bis-(dipyrrinato)zinc(II) Complexes. Eight dissymmetric bis-(dipyrrinato)zinc(II) complexes **1a–h** were synthesized (Figure 1a). Each has two different dipyrrinato ligands derived from one plain dipyrrin (**4**) and one π-expanded dipyrrin (**5a–h**). Scheme S1 illustrates the synthetic procedure for **5a–h**. Corresponding symmetric reference complexes **2a–h** and **3** were also prepared using dipyrrins **4** and **5a–h**. Bulky substituents on a chromogenic core are pros and cons: They protect the core from quenching by self-aggregation and solvation,[15] while intramolecular collisions may activate non-radiative decays.[16] However, the basic structure of the π-expanded dipyrrinato ligand involves the introduction of styryl groups at the α position: the simplest one corresponds to ligand **5a**. This type of modifications narrows the $^1\pi$–π^* gap of the dipyrrinato ligand considerably.[17] The variations of the π-expanded dipyrrinato ligand (**5b–h**) include (1) substituting the arene of the styryl group with electron donating ones such as 2-thienyl and 2,4-dimethoxyphenyl groups (**5b,c**); (2) extending the styryl group to a 4-phenylbuta-1,3-dienyl group (**5d**); and (3) adding (4-methylphenyl)ethynyl groups at the β position (**5f**). Combinations of (1) and (2) (**5e**) and (1) and (3) (**5g,h**) were also synthesized. Figure 1b shows a general procedure for synthesizing the dissymmetric complexes. A mixture of plain dipyrrin **4**, π-expanded dipyrrin **5a–h**, and zinc acetate was stirred in dichloromethane at room temperature. The dissymmetric complex was separated by gel permeation chromatography, and purified by recrystallization. Symmetric complexes **2a**, **2c**, **2d**, and **2f–h** were retrieved as byproducts, whereas **2b**, **2e**, and **3** were synthesized separately. The symmetric and dissymmetric complexes were identified by high-resolution mass spectrometry and ^{1}H and ^{13}C NMR spectroscopy. For example, the ^{1}H NMR spectrum of each

DOI: 10.1021/jacs.6b02128
J. Am. Chem. Soc. 2016, 138, 5666–5677

dissymmetric complex appears different from that of each corresponding symmetric complex (Figures S3–S10), which indicates that the dissymmetric complex resists disproportionation into the symmetric complexes.

Single-crystal X-ray structure analysis. The dissymmetry of the complexes was confirmed by single-crystal X-ray diffraction analysis for **1e** (Figure 1c). The crystal structure of symmetric reference complex **2a** was also determined (Figure 1d). Their crystallographic data are summarized in Tables S1 and S2, and the CIF files are provided for 1e and 2a. Dissymmetric **1e** possesses two different dipyrrinato ligands (**4** and **5e**), whereas **2a** has a pair of π-expanded dipyrrinato ligands (**5a**). In both cases, the four pyrrole nitrogen atoms coordinate to the zinc center in a slightly distorted tetrahedron. The dihedral angles for the two planes, defined by N(1) − Zn−N(2) and N(3)−Zn−N(4), are 84.80° in **1e** and 80.39° in **2a**. The deviation from orthogonality was presumably caused by the crystal packing. Symmetric complex **2a** shows intramolecular steric repulsion between the two bulky π-expanded dipyrrinato ligands, which leads to greater deviation from orthogonality than in **1e**. The distances between the zinc center and the pyrrole nitrogen are 1.971−1.980 Å in **1e** and 1.962−1.979 Å in **2a**. The dihedral angles and coordination bond lengths are consistent with those reported for bis(dipyrrinato)-zinc(II) complexes.[10,12a,18]

Photophysical Properties. The optical properties of dissymmetric bis(dipyrrinato)zinc(II) complexes **1a–h**, and corresponding symmetric complexes **2a–h** and **3** were explored by UV/vis, PL, and PL lifetime spectroscopy. Figure 2 shows

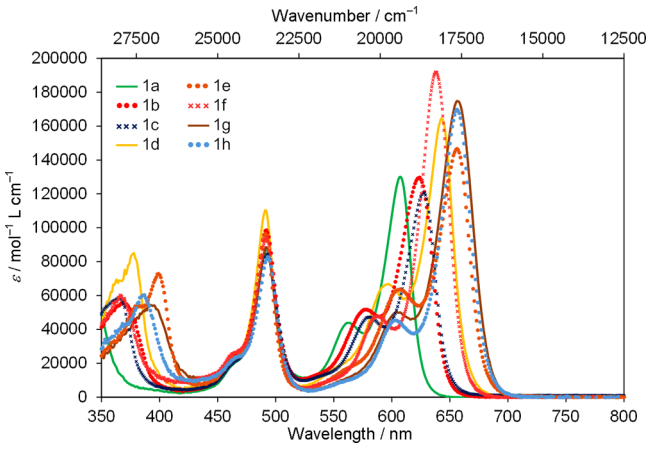

Figure 2. UV/vis spectra of dissymmetric complexes **1a–h** in toluene.

the UV/vis spectra of dissymmetric complexes **1a–h** in toluene, and the spectra of the symmetric complexes are given in Figure S11. Figure 3 overlays the UV/vis and PL spectra of corresponding dissymmetric and symmetric complexes (e.g., **1a**, **2a**, and **3** in Figure 3a). The numerical data are listed in Table 1, including the PL quantum yields (ϕ_{PL}) and lifetimes (τ), and several parameters in toluene or dichloromethane. The photographs in Figure 4 show solutions of the complexes under ambient conditions and under 365 nm UV illumination. In the UV/vis spectra, dissymmetric complexes **1a–h** share a common electronic band at around 490 nm. This corresponds to the $^1\pi-\pi^*$ transition of plain dipyrrinato ligand **4**, judging from the absorption spectrum of symmetric complex **3** containing only dipyrrinato ligand **4**. The dissymmetric complexes show another distinctive electronic band at 530−700 nm. Comparison with symmetric complexes **2a–h** suggests this band can be assigned to the $^1\pi-\pi^*$ transition of π-expanded dipyrrinato ligands **5a–h**.

Next we discuss PL, which is induced by the photoexcitation with the $^1\pi-\pi^*$ band. The two different $^1\pi-\pi^*$ bands derived from the plain and π-expanded dipyrrinato ligands in the dissymmetric complexes were photoexcited independently. Symmetric complexes **2a–h** and **3** were luminescent, but showed only weak or modest PL (ϕ_{PL} = 0.03−0.21) in nonpolar toluene (dielectric constant ε_s = 2.4), which was quenched (ϕ_{PL} = 0−0.03) in more polar dichloromethane (ε_s = 9.1). However, dissymmetric complexes **1a–h** feature two distinct luminescent characteristics. First, PL was emitted exclusively from the $^1\pi-\pi^*$ state of π-expanded dipyrrinato ligands **5a–h**, even when the $^1\pi-\pi^*$ band of plain dipyrrinato ligand **4** was photoexcited. In addition, ϕ_{PL} was constant irrespective of which $^1\pi-\pi^*$ band was photoexcited. This indicates that the dissymmetric complexes undergo quantitative energy transfer from the plain dipyrrinato ligand to the π-expanded dipyrrinato ligand. As a result, the quantitative energy transfer realized large pseudo-Stokes shifts of 4100−5400 cm^{-1}. Second, the ϕ_{PL} values of the dissymmetric complexes are always greater than those of the corresponding symmetric ones. Dissymmetric complexes **1a–h** fluoresced brightly or modestly in toluene (ϕ_{PL} = 0.16−0.72), and maintained their fluorescence in more polar dichloromethane (ϕ_{PL} = 0.09−0.71). The superior PL ability of the dissymmetric complexes is also shown in Figure 4. Of note is dissymmetric complex **1g**, which featured bright luminescence (ϕ_{PL} = 0.62−0.69) even in more polar acetone (ε_s = 21.4) and ethanol (ε_s = 24.3) (Table 1). The PL maxima (λ_{PL}) of **1a–h** ranged from 616 to 671 nm, covering the red and part of the NIR region. A further argument is described in the Discussion section.

Electrochemistry. The electrochemical properties of the nine symmetric complexes (**2a–h** and **3**) were studied by cyclic voltammetry, to investigate the energy levels of the π and π^* orbitals of the dipyrrinato ligands (Figure 5 and Table 2). Electrochemistry for bis(dipyrrinato)metal(II) and tris-(dipyrrinato)metal(III) complexes is rarely reported.[1a,5a,19] When swept in the positive direction, each complex showed two reversible one-electron redox waves, assignable to the one-electron oxidation of the π orbital of each dipyrrinato ligand. The split between the first and second redox waves arose from Coulombic repulsion,[20] rather than an intrinsic difference in the energy level. The orthogonality of the two dipyrrinato ligands (Figure 1d) rules out a contribution from electronic communication.[21] Similarly, the first and second one-electron reductions were split, except for **2d,e** and **3**. This split probably also arose from Coulombic repulsion. Complexes **2d** and **2e** showed small or negligible splitting of the first and second reductions. The two complexes both feature 4-arylbuta-1,3-dienyl groups at the α position, which might induce a structural change in the second reduction step and cause a positive shift to the second reduction potential. The second reduction wave of **3** was out of the potential window. Therefore, the redox potentials for the first oxidation and reduction represent the energy levels of the π and π^* orbitals of each dipyrrinato ligand, with the energy gap between the two potentials being consistent with λ_{abs} and/or λ_{PL} in dichloromethane. Note that **2b** showed a four-electron redox wave additionally, whereas **2e** and **2g** displayed an additional two-electron redox wave. The three complexes share electron-rich 2,4-dimethoxyphenyl

DOI: 10.1021/jacs.6b02128
J. Am. Chem. Soc. 2016, 138, 5666−5677

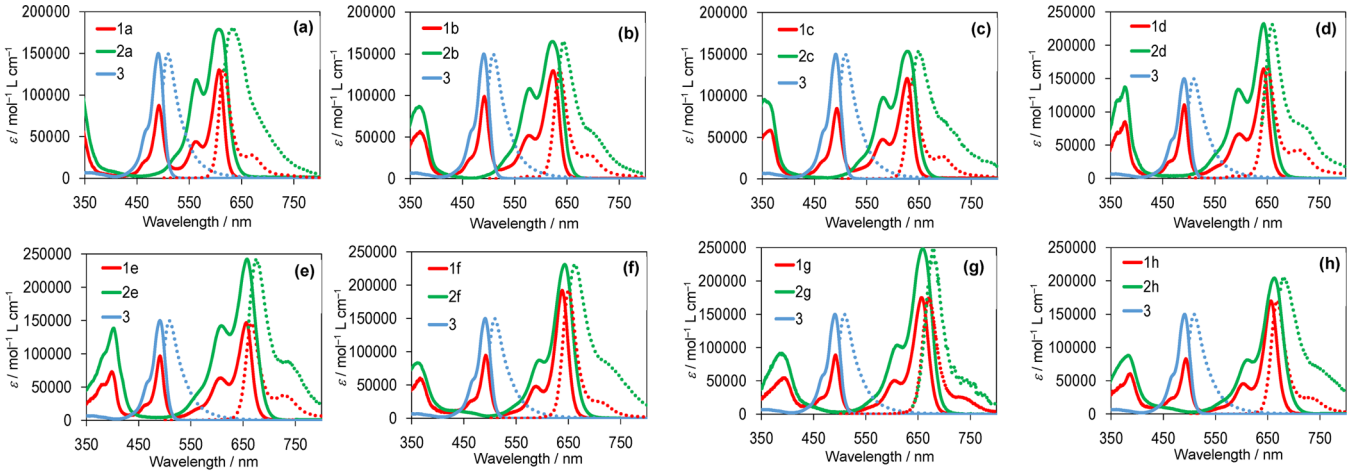

Figure 3. Overlays of UV/vis (solid lines) and normalized PL (dotted lines) spectra of dissymmetric complexes **1a**–**h** (red) and their corresponding symmetric complexes **2a**–**h** (green) and **3** (blue) in toluene: (a) **1a**, **2a**, and **3**; (b) **1b**, **2b**, and **3**; (c) **1c**, **2c**, and **3**; (d) **1d**, **2d**, and **3**; (e) **1e**, **2e**, and **3**; (f) **1f**, **2f**, and **3**; (g) **1g**, **2g**, and **3**; and (h) **1h**, **2h**, and **3**.

Table 1. Photophysical Properties of Dissymmetric Complexes 1a–h and Corresponding Symmetric Complexes 2a–h and 3

	λ_{abs} (nm)[a]			λ_{PL}(nm)		ϕ_{PL}		τ (ns)	
	toluene	CH_2Cl_2	ε_{abs} ($\times 10^4$ M^{-1} cm^{-1})[b]	toluene	CH_2Cl_2	toluene	CH_2Cl_2	toluene	CH_2Cl_2
1a	492	490	8.7	616	614	0.70	0.29	3.2	3.1
	607	605	13	616	614	0.66	0.29	3.3	3.2
1b	492	490	9.9	636	635	0.69	0.38	3.0	2.8
	624	621	13	636	635	0.69	0.41	3.1	2.8
1c	493	491	8.5	637	635	0.50	0.24	2.3	2.2
	627	624	12	637	635	0.46	0.26	2.4	2.2
1d	491	489	11	651	650	0.16	0.13	0.83	0.77
	643	640	16	651	650	0.16	0.12	0.85	0.78
1e	491	490	9.7	666	665	0.19	0.16	0.87	0.79
	656	654	15	666	665	0.18	0.15	0.89	0.80
1f	492	491	9.4	650	648	0.70	0.11	3.2	2.2
	638	635	19	650	647	0.63	0.09	3.2	2.3
1g	492	491	8.9	671	669	0.72	0.71 (0.69,[c] 0.66[d])	3.1	3.4
	656	652	18	671	669	0.72	0.70 (0.65,[c] 0.62[d])	3.2	3.4
1h	493	491	8.3	667	665	0.60	0.10	3.1	1.7
	656	651	17	667	665	0.56	0.11	3.2	1.8
2a	607	603	18	630	623	0.08	0.01	5.8	[e]
2b	622	621	16	644	639	0.04	<0.01	4.7	[e]
2c	628	625	15	648	641	0.03	<0.01	3.9	[e]
2d	643	640	23	659	655	0.05	0.01	2.9	0.85
2e	657	656	24	675	673	0.04	<0.01	[e]	[e]
2f	643	639	23	662	655	0.21	0.02	4.4	3.5
2g	660	657	25	680	673	0.07	0.02	3.8	3.0
2h	662	658	20	678	673	0.12	0.03	3.6	[e]
3	491	489	15	509	508	0.18	<0.01	2.4	[e]

[a]As for the $^1\pi$–π^* bands of the dipyrrinato ligands. [b]In toluene. [c]In acetone. [d]In ethanol. [e]Not measured because of a weak signal.

groups; therefore, the additional redox wave may be associated with the oxidation of the 2,4-dimethoxyphenyl group.

DISCUSSION

As anticipated, dissymmetric complexes **1a**–**h** showed consistently brighter luminescence than corresponding symmetric complexes **2a**–**h**. In addition, the dissymmetric complexes underwent quantitative intramolecular and interligand energy transfer from plain dipyrrinato ligand **4** to π-expanded dipyrrinato ligands **5a**–**h**, achieving large pseudo-Stokes shifts (4100–5400 cm^{-1}). The driving force for the quantitative energy transfer is derived from, as experimentally elucidated in UV/vis and PL spectroscopy, the excitation energy gap between plain dipyrrinato ligand **4** (wider) and π-expanded dipyrrinato ligands **5a**–**h** (narrower). The large pseudo-Stokes shift may differentiate dissymmetric bis(dipyrrinato)zinc(II) complexes from BODIPYs with very small Stokes shifts (~500 cm^{-1}).[1] Of the eight complexes, complex **1a** showed the least red-shifted PL (λ_{PL} = 614–616 nm). The PL quantum yields (ϕ_{PL} = 0.66–0.70 in toluene and 0.29 in dichloromethane) were far greater than those of corresponding symmetric complex **2a** (ϕ_{PL} = 0.08 and 0.01). The higher ϕ_{PL} in **1a**

DOI: 10.1021/jacs.6b02128
J. Am. Chem. Soc. 2016, 138, 5666–5677

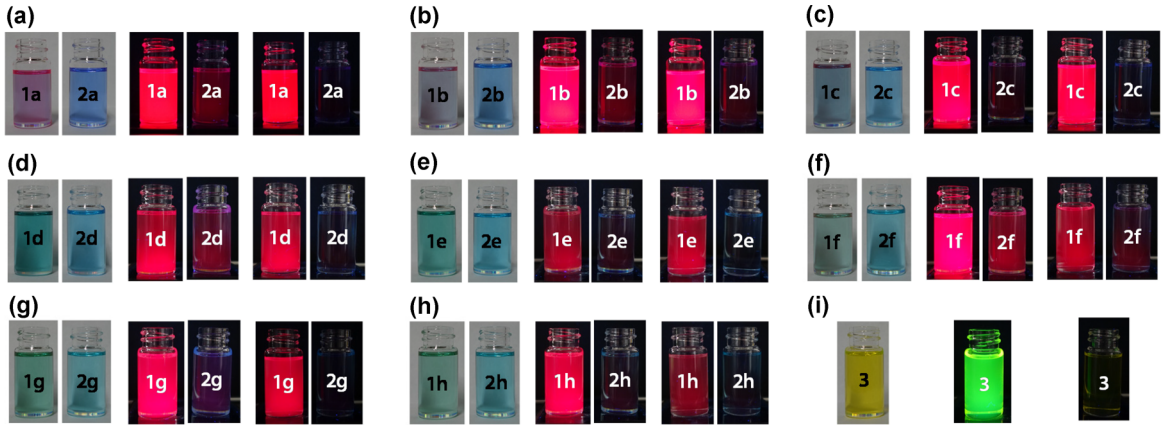

Figure 4. Photographs of toluene solution of complexes (left); their PL upon illumination with 365 nm UV light in toluene (center) and dichloromethane (right): (a) **1a** and **2a**; (b) **1b** and **2b**; (c) **1c** and **2c**; (d) **1d** and **2d**; (e) **1e** and **2e**; (f) **1f** and **2f**; (g) **1g** and **2g**; (h) **1h** and **2h**; and (i) **3**. The optical densities at 365 nm are fixed at similar values for all samples.

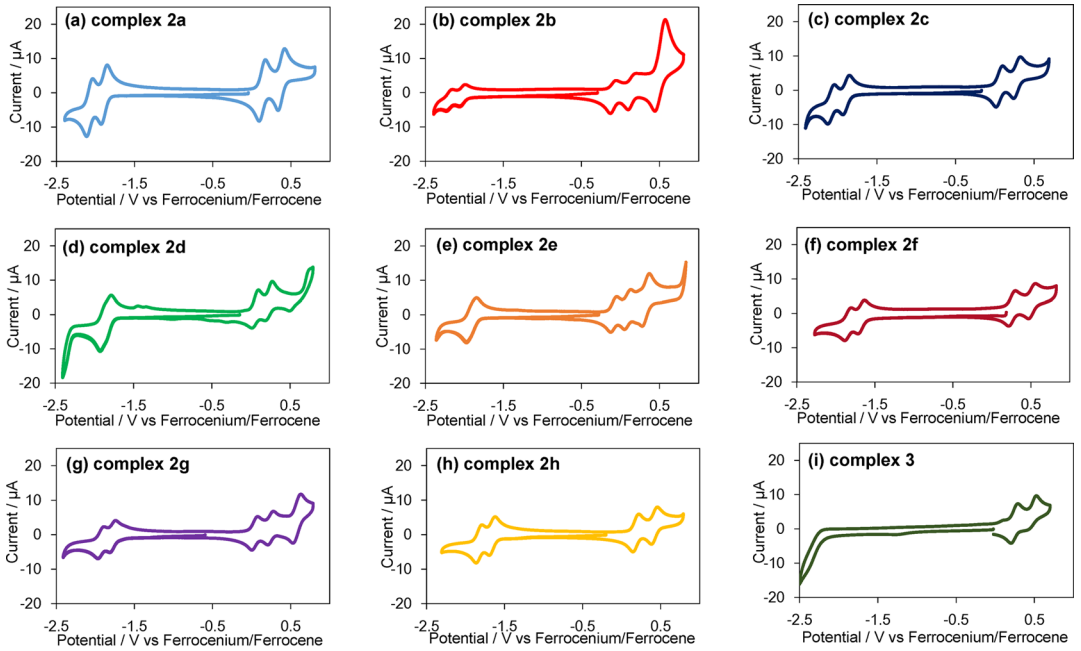

Figure 5. Cyclic voltammograms for symmetric complexes **2a–h** and **3** (0.5 mM) in 0.1 M *n*-Bu_4NPF_6/dichloromethane. Scan rate = 0.1 V s^{-1}.

Table 2. Redox Potentials of Symmetric Complexes 2a–h and 3

	E_{red}[a]/V	E_{ox}[b]/V	HOMO–LUMO gap/eV (λ/nm)
2a	−2.07, −1.89	0.14, 0.38	2.03 (611)
2b	−2.19, −2.02	−0.09, 0.15, 0.51	1.93 (642)
2c	−2.08, −1.89	0.06, 0.29	1.95 (636)
2d	−1.85	0.06, 0.23	1.91 (649)
2e	−1.90	−0.08, 0.09, 0.33	1.82 (681)
2f	−1.84, −1.67	0.26, 0.52	1.93 (642)
2g	−1.93, −1.78	0.04, 0.24, 0.58	1.82 (681)
2h	−1.82, −1.66	0.19, 0.42	1.85 (670)
3	−2.35[c]	0.28, 0.53[c]	2.62 (473)

[a]Halfwave potentials vs ferrocenium/ferrocene for reductions. [b]Halfwave potentials for oxidations. [c]From differential pulse voltammetry.

may be explained by our charge separation hypothesis (Figure 6).[12a] Figure S12a shows the frontier orbital ordering of **1a**. The molecular orbitals were drawn by DFT calculation, and their energy levels were determined from electrochemical measurements for corresponding symmetric complexes **2a** and **3** (Figure 5 and Table 2). The π-expansion localized the highest occupied molecular orbital (HOMO) and lowest unoccupied molecular orbital (LUMO) on π-expanded dipyrrinato ligand **5a**, whereas the HOMO−1 and LUMO+1 had contributions from plain dipyrrinato ligand **4** exclusively. In this scheme, quenching charge-separated states are disfavored compared with the emissive $^1\pi$–π^* excited state (Figure 6a), in contrast to the symmetric complex, in which Thompson and co-workers[10] showed that the $^1\pi$–π^* excited state competes with the charge-separated states, especially in polar solvents (Figure 6b). As a result, the dissymmetric complex enjoys higher ϕ_{PL} than the symmetric one, the difference of which is highlighted in polar solvents.

We designed molecules based on **1a** to pursue more PL red-shifts and better ϕ_{PL}. The styryl group on the π-expanded dipyrrinato ligand was substituted with a 2,4-dimethoxystyryl

DOI: 10.1021/jacs.6b02128
J. Am. Chem. Soc. 2016, 138, 5666–5677

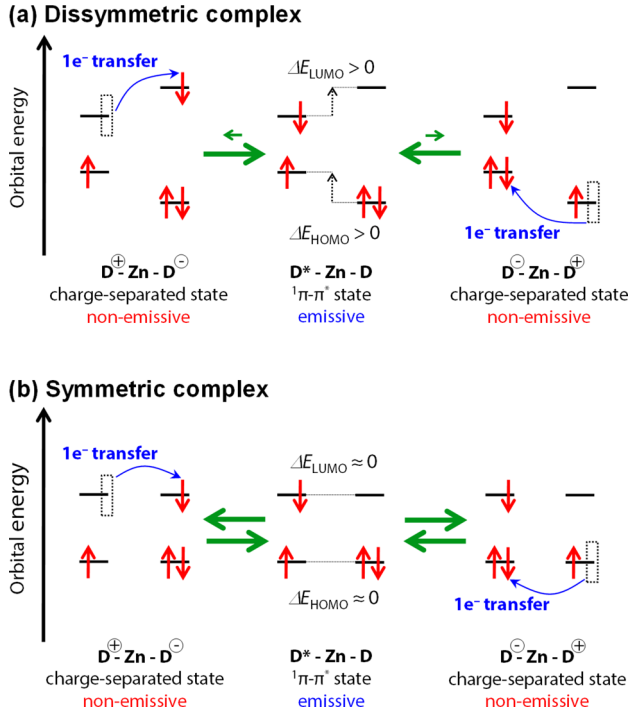

Figure 6. Schematic illustrations of plausible thermal equilibria among the two non-emissive symmetry-breaking charge-separated states (D^+-Zn-D^- and D^-Zn-D^+) and the emissive $^1\pi-\pi^*$ excited state localized on the left-hand dipyrrinato ligand (**D***−**Zn**−**D**) for (a) dissymmetric complex and (b) symmetric complex. ΔE_{HOMO} denotes the energy gap between HOMO and HOMO−1, and ΔE_{LUMO} stands for that between LUMO+1 and LUMO. **Zn** and **D** represent the Zn^{2+} center and dipyrrinato ligand, respectively.

group in complex **1b**, whose electronic structure (Figure S12b) indicated that the HOMO and LUMO were both destabilized compared with those in **1a**, although the HOMO was more destabilized. As a result, the HOMO−LUMO gap narrowed, realizing a red-shift in the λ_{PL} (635−636 nm) with high ϕ_{PL} (0.69 in toluene and 0.38−0.41 in dichloromethane). Corresponding symmetric complex **1b** exhibited very low ϕ_{PL} (0.04 in toluene and ∼0 in dichloromethane). Substitution with 2-thienyl groups in complex **1c** also red-shifted the PL (λ_{PL} = 635−637 nm). This substitution destabilized only the HOMO, contributing to the HOMO−LUMO gap narrowing (Figures S12c). The PL intensity of **1c** (ϕ_{PL} = 0.46−0.50 in toluene and 0.24−0.26 in dichloromethane) was greater than that of corresponding symmetric complex **5c** (ϕ_{PL} = 0.03 in toluene and ∼0 in dichloromethane), but was smaller than that of **1a** or **1b**.

We extended the styryl group of complex **1a** to a 4-phenylbuta-1,3-dienyl group so as to create complex **1d**. This modification resulted in further π-expansion, leading to greater HOMO−LUMO gap narrowing (λ_{PL} = 650−651 nm, Figure S12d). The PL quantum yields (ϕ_{PL} = 0.16 in toluene and 0.12−0.13 in dichloromethane) were larger than those of corresponding symmetric complex **2d** (ϕ_{PL} = 0.05 in toluene and 0.01 in dichloromethane), but smaller than those of **1a**−**c**. Considering that the PL lifetime (τ) of complex **1d** was shortened in both toluene and dichloromethane compared with those of **1a**−**c**, the 4-phenylbuta-1,3-dienyl group appeared to provide an additional thermal deactivation pathway, probably because of its flexible structure and resultant vibrations. The behavior of dissymmetric complex **1e** with a 4-(2,4-dimethoxyphenyl)buta-1,3-dienyl group (λ_{PL} = 665−666 nm, ϕ_{PL} = 0.18−0.19 in toluene and 0.15−0.16 in dichloromethane, Figure S12e) and its corresponding symmetric complex, **2e** (ϕ_{PL} = 0.04 in toluene and ∼0 in dichloromethane), may also be explained in the same way.

Another π-expansion strategy involved introducing a (4-methylphenyl)ethynyl group to the β position of **1a**−**c**, to create dissymmetric complexes **1f**−**h**. This strategy worked well, resulting in large red-shifts in the PL (λ_{PL} = 647−650, 669−671, and 665−667 nm for **1f**−**h**, respectively). Complexes **1f** and **1g** had similar molecular structures, differing only in the methoxy groups, and they showed similar PL quantum yields and lifetimes in toluene (ϕ_{PL} = 0.63−0.70 and τ = 3.2 ns for **1f**

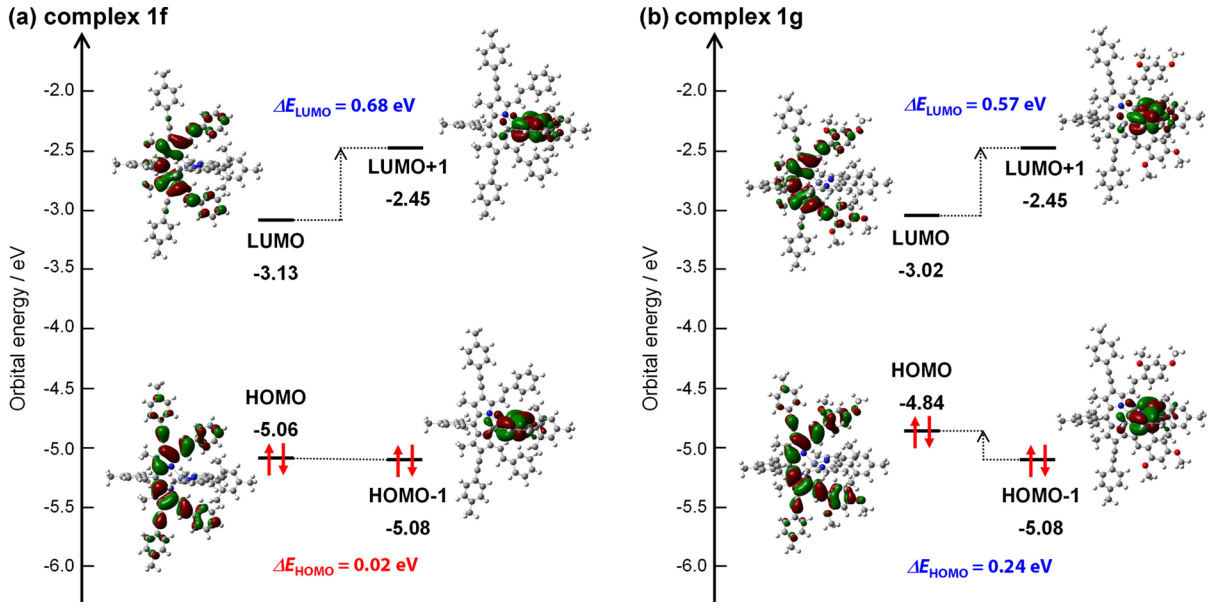

Figure 7. Frontier orbital ordering of (a) **1f** and (b) **1g** estimated by cyclic voltammetry and DFT calculations. The redox potential was converted into the vacuum level according to a previous literature.[22]

DOI: 10.1021/jacs.6b02128
J. Am. Chem. Soc. 2016, 138, 5666−5677

and ϕ_{PL} = 0.72 and τ = 3.1−3.2 ns for **1g**). However, they showed a significant difference in more polar solvent, dichloromethane. **1f** suffered a significant loss of ϕ_{PL}, whereas **1g** retained its bright luminescence (ϕ_{PL} = 0.09−0.11 and τ = 2.2−2.3 ns for **1f** and ϕ_{PL} = 0.70−0.71 and τ = 3.4 ns for **1g**). These results suggest that **1f** has an additional quenching channel in dichloromethane, which is not available in **1g**. The discrepancy between dissymmetric complexes **1f** and **1g** may be well explained by our charge separation hypothesis (Figure 6). Figure 7 shows the frontier orbital ordering in **1f** and **1g**. Because both the styryl and the arylethynyl groups are electron withdrawing, the two kinds of π-expansion affect the π^* orbital chiefly, providing significant stabilization. As a result, complex **1f** shows a large energy gap between the LUMO and LUMO+1 (ΔE_{LUMO} = 0.68 eV), whereas the HOMO and HOMO−1 are virtually degenerated (ΔE_{HOMO} = 0.02 eV, Figure 7a). The scheme in Figure 6a indicates that the electronic structure allows **1f** to prevent charge separation through one-electron transfer from the LUMO to LUMO+1; however, charge separation involved in the one-electron transfer from the HOMO−1 to HOMO is not hindered by the small energy barrier. The higher polarity stabilizes the polarized species, which may explain the additional quenching pathway of complex **1f** in dichloromethane, and thus the reduced ϕ_{PL} and τ therein. In contrast, the electron donating methoxy group in complex **1g** destabilizes the π orbital greatly and the π^* orbital slightly (Figure 7b). As a result, sufficient energy gaps between the HOMO and HOMO−1 (ΔE_{HOMO} = 0.24 eV), and the LUMO+1 and LUMO (ΔE_{LUMO} = 0.57 eV) are confirmed. This electronic structure allows complex **1g** to avoid charge separation and retain its bright luminescence, even in polar dichloromethane. Dissymmetric **1f**, **1g**, and **1h** (ϕ_{PL} = 0.56−0.60 in toluene and 0.10−0.11 in dichloromethane, Figure S12f) had higher PL efficiencies than corresponding symmetric complexes **2f** (ϕ_{PL} = 0.21 and 0.02), **2g** (ϕ_{PL} = 0.07 and 0.02), and **2h** (ϕ_{PL} = 0.12 and 0.03).

Of the eight dissymmetric complexes, **1g** had the best PL properties, and maintained high efficiencies in significantly polar solvents [ϕ_{PL} = 0.65−0.69 in acetone (ε_s = 21.4); ϕ_{PL} = 0.62−0.66 in ethanol (ε_s = 24.3), Table 1]. Therefore, the dissymmetry solves the drawback of bis(dipyrrinato)zinc(II) complexes as luminophores, significant PL quench in polar solvent. Note that the ϕ_{PL} values of **1g** were higher than or comparable to those of BODIPYs fluorescing at similar wavelengths (Figure S13).[23]

CONCLUSIONS

Eight dissymmetric bis(dipyrrinato)zinc(II) complexes, comprising a plain dipyrrinato ligand and a π-expanded dipyrrinato ligand, were designed and synthesized. Corresponding symmetric complexes were also fabricated as references. The complexes were characterized, and single-crystal XRD analysis confirmed that they were dissymmetric or symmetric as expected. The dissymmetric complexes featured distinctive photophysical properties, such as PL in the red and NIR region, with much higher quantum efficiencies than their symmetric counterparts. The best PL property was achieved in complex **1g**, whose λ_{PL} reached 671 nm, and maintained high ϕ_{PL} (0.62−0.72) in toluene and dichloromethane, and in highly polar acetone and ethanol. The dissymmetry improved the fatal drawback of bis(dipyrrinato)zinc(II) complexes, significant PL quench in polar solvent. The bright luminescence of **1g** was better than or comparable to those of π-expanded BODIPYs with similar λ_{PL}. In addition, the dissymmetric complexes possessed large pseudo-Stokes shifts (4100−5400 cm^{-1}): Photoexcitation with the plain dipyrrinato ligand induced quantitative intramolecular and interligand energy transfer, such that luminescence was emitted exclusively from the π-expanded dipyrrinato ligand. The large pseudo-Stokes shift may be one of the characteristics of dissymmetric bis(dipyrrinato)zinc(II) complexes as luminophores, because BODIPYs typically possess very small Stokes shifts (~500 cm^{-1}). Electrochemical measurements quantified the energy level of the highest π and lowest π^* orbitals of each dipyrrinato ligand, proving that the dissymmetric complexes possessed frontier orbital ordering suitable for bright luminescence, which destabilized quenching charge-separated states competing with the emissive $^1\pi$−π^* excited state. The most striking comparison was provided by the structurally similar complexes **1f** and **1g**, which possessed similar ϕ_{PL} and τ in nonpolar toluene, but different values in polar dichloromethane. The ϕ_{PL} and τ values for **1g** in dichloromethane were similar to those in toluene, whereas those for **1f** were much smaller in dichloromethane. This difference was explained by the charge separation hypothesis and frontier orbital ordering. The present research demonstrates the universality of our dissymmetric design for bis(dipyrrinato)zinc(II) complexes with bright luminescence reaching the NIR region. These results also demonstrate the usefulness of bis(dipyrrinato)zinc(II) complexes as photofunctional molecular materials such as luminophores and sensitizers.

EXPERIMENTAL SECTION

Materials. Symmetric complex **3** and plain dipyrrin **4**,[12a] and (*E*)-3-(2,4-dimethoxyphenyl)acrylaldehyde[24] were synthesized according to previous reports. Tetra-*n*-butylammonium hexafluorophosphate as a supporting electrolyte was purified by recrystallization from ethanol, which was dried in vacuo. Solvents for organic syntheses were purified using a solvent purification system (Ultimate Solvent System, Nikko Hansen & Co., Ltd.). The other chemicals were general grades and were used as received. All procedures were conducted under a nitrogen condition otherwise stated.

Apparatus. ^{1}H (500 MHz) and ^{13}C (125 MHz) nuclear magnetic resonance (NMR) data were collected in $CDCl_3$ on a Bruker US500 spectrometer. Tetramethylsilane (δ_H = 0.00) was used as an internal standard for the ^{1}H NMR spectra, and $CDCl_3$ (δ_C = 77.00) was used as an internal standard for the ^{13}C NMR spectra, respectively. Fast atom bombardment mass spectrometry (FAB-MS) and electrospray ionization time-of-flight mass spectrometry were conducted using a JEOL JMS-700 MStation and Micromass LCT Premier XE mass spectrometer, respectively. Absorption spectra were measured with a JASCO V-570 spectrometer. Fluorescence spectra were measured with a HITACHI F-45 00 spectrometer. Preparative gel permeation liquid chromatography was performed by LC-918 equipped with JAIGEL 1H and H3 columns (Japan Analytical Industry), using chloroform as eluent. Absolute photo luminescent quantum yields were collected with HAMAMATSU C9920-01. Fluorescence lifetime measurements were performed using a Hamamatsu Photonics Quantaurus-Tau C11367-02.

Synthesis of 5a. To a *N*,*N*-dimethylformamide solution (15 mL) of dipyrrin **4** (159 mg, 0.50 mmol) and benzaldehyde (0.21 mL, 2.0 mmol), acetic acid (1.0 mL) and piperidine (1.0 mL) were added and the reaction mixture was heated to reflux for 1 h. Further benzaldehyde (0.10 mL, 1.0 mmol) was added to the mixture and stirred for 30 min. After the consumption of **4** was confirmed by TLC, the mixture was cooled to room temperature. The solution was diluted with ethyl acetate and washed with brine. The organic layer was dried over Na_2SO_4 and evaporated. The reaction mixture was processed by column chromatography (alumina, dichloromethane/hexane =1/4) followed by recrystallization from dichloromethane/methanol to give

DOI: 10.1021/jacs.6b02128
J. Am. Chem. Soc. 2016, 138, 5666−5677

the pure product as a dark purple solid (179 mg, 72%). ^{1}H NMR (500 MHz, $CDCl_3$): δ = 14.11 (br s, 1H), 7.55 (d, J = 7.3 Hz, 4H), 7.38 (t, J = 7.6 Hz, 4H), 7.29 (t, J = 7.3 Hz, 2H), 7.20 (d, J = 16 Hz, 2H), 7.13 (d, J = 16 Hz, 2H), 6.94 (s, 2H), 6.37 (s, 2H), 2.34 (s, 3H), 2.14 (s, 6H), 1.38 (s, 6H); ^{13}C NMR (125 MHz, $CDCl_3$): δ = 150.72, 140.30, 138.56, 137.86, 137.45, 137.10, 135.80, 133.64, 131.74, 128.76, 128.65, 128.01, 126.80, 121.09, 118.61, 21.21, 19.71, 13.82; HR-FAB-MS (m/z): $[M + H]^+$, calculated for $C_{36}H_{35}N_2^+$, 495.2801; found, 495.2776.

Synthesis of 5b. To a *N,N*-dimethylformamide solution (20 mL) of dipyrrin **4** (161 mg, 0.50 mmol) and 2,4-dimethoxybenzaldehyde (338 mg, 2.0 mmol), acetic acid (1.0 mL) and piperidine (1.0 mL) were added and the reaction mixture was heated to reflux for 4 h. After cooling the solution, the solution was diluted with ethyl acetate and washed with brine. The organic layer was dried over Na_2SO_4 and evaporated. The dark purple solid was recrystallized from hexane/dichloromethane to give the desired product as a black solid (160 mg, 52%). ^{1}H NMR (500 MHz, $CDCl_3$): δ = 14.17 (br s, 1H), 7.56 (d, J = 8.5 Hz, 2H), 7.49 (d, J = 16 Hz, 2H), 7.03 (d, J = 16 Hz, 2H), 6.92 (s, 2H), 6.52 (dd, J = 8.5, 2.6 Hz, 2H), 6.45 (d, J = 2.6 Hz, 2H), 6.34 (s, 2H), 3.84 (s, 6H), 3.77 (s, 6H), 2.34 (s, 3H), 2.13 (s, 6H), 1.37 (s, 6H); ^{13}C NMR (125 MHz, $CDCl_3$): δ = 160.82, 158.33, 151.43, 139.71, 138.22, 137.60, 136.18, 135.99, 133.97, 128.51, 127.30, 126.35, 119.63, 119.31, 118.24, 105.08, 98.34, 55.44 (2C), 21.21, 19.74, 13.79; HR-FAB-MS (m/z): M^+, calculated for $C_{40}H_{42}N_2O_4^+$, 614.3145; found, 614.3122.

Synthesis of 5c. 2-Thiophenecarboxaldehyde (673 mg, 6.0 mmol) was added to a solution of **4** (478 mg, 1.5 mmol), piperidine (0.75 mL) and acetic acid (0.75 mL) in DMF (25 mL). The reaction mixture was stirred for 16 h at 90 °C and changed color to purple. Hexane (30 mL) and ethyl acetate (30 mL) were added and the reaction mixture was extracted with water (100 mL). The aqueous phase was extracted with a 1:1 mixture of hexane and ethyl acetate (60 mL) and the combined organic phases were washed with water. After drying over sodium sulfate, all volatiles were removed *in vacuo*. The dark blue residue was recrystallized from dichloromethane/methanol at −30 °C to give 496 mg of the pure product as a dark blue solid. Evaporation of the solvent from the filtrate and washing the residue with a small amount of methanol yielded another 51 mg of the product (total yield: 547 mg, 72%). ^{1}H NMR (500 MHz, $CDCl_3$, 25 °C): δ = 14.09 (br s, 1H), 7.29 (d, J = 16 Hz, 2H), 7.27 (d, J = 3.9 Hz, 2H), 7.13 (d, J = 3.4 Hz, 2H), 7.05 (dd, J = 3.7, 3.6 Hz, 2H), 6.94 (d, J = 16 Hz, 2H), 6.94 (s, 2H), 6.32 (s, 2H), 2.35 (s, 3H), 2.13 (s, 6H), 1.37 (s, 6H); ^{13}C NMR (125 MHz, $CDCl_3$): δ = 150.20, 142.90, 140.29, 138.76, 137.86, 137.01, 135.85, 133.63, 128.63, 127.87, 126.90, 125.22, 124.55, 120.64, 118.59, 21.21, 19.70, 13.79; HR-ESI-TOF-MS (m/z): M^+, calculated for $C_{32}H_{30}N_2S_2^+$, 506.1850; found, 506.1804.

Synthesis of 5d. To a *N,N*-dimethylformamide solution (20 mL) of dipyrrin **4** (160 mg, 0.50 mmol) and cinnamaldehyde (0.26 mL, 2.1 mmol), acetic acid (1.0 mL) and piperidine (1.0 mL) were added and the reaction mixture was heated to 80 °C for 1.5 h. After cooling the solution, the solution was diluted with ethyl acetate and washed with brine. The organic layer was dried over Na_2SO_4 and evaporated. The black solid was recrystallized from methanol/dichloromethane to give the desired product as a dark purple solid (43 mg, 16%). ^{1}H NMR (500 MHz, $CDCl_3$): δ = 14.07 (br s, 1H), 7.43 (d, J = 7.3 Hz, 4H), 7.32 (t, J = 7.3 Hz, 4H), 7.24 (t, J = 7.6 Hz, 2H), 7.11−6.97 (m, 4H), 6.93 (s, 2H), 6.83 (d, J = 15 Hz, 4H), 6.29 (s, 2H), 2.34 (s, 3H), 2.12 (s, 6H), 1.37 (s, 6H); ^{13}C NMR (125 MHz, $CDCl_3$): δ = 150.54, 140.25, 139.07, 137.84, 137.14, 136.79, 135.85, 134.22, 133.65, 132.34, 129.21, 128.67, 128.63, 127.78, 126.62, 124.88, 119.23, 21.22, 19.75, 13.80; HR-FAB-MS (m/z): $[M + H]^+$, calculated for $C_{40}H_{39}N_2^+$, 547.3113; found, 547.3104.

Synthesis of 5e. To a *N,N*-dimethylformamide solution (10 mL) of dipyrrin **4** (156 mg, 0.49 mmol) and 4 Å molecular sieves (3 g), acetic acid (1.0 mL) and piperidine (1.0 mL) were added and the reaction mixture was heated to 80 °C. A *N,N*-dimethylformamide solution (15 mL) of (*E*)-3-(2,4-dimethoxyphenyl)acrylaldehyde (570 mg, 3.0 mmol) was added dropwise over 3 h to the stirred mixture and stirred for additional 2 h. After the consumption of **4** was confirmed by TLC, the mixture was cooled to room temperature. The solution was diluted with ethyl acetate and washed with brine. The organic layer was dried over Na_2SO_4 and evaporated. The reaction mixture was processed by column chromatography (alumina, diethyl ether/hexane =1/1) to give the crude product as a dark blue solid (171 mg, 52%), which was used in the next reaction without further purification.

Synthesis of 1,9-bis[(*E*)-2-phenylethenyl]-2,8-diiodo-3,7-dimethyl-5-(2,4,6-trimethylphenyl)dipyrrin (6). Iodine (308 mg, 1.2 mmol) and iodic acid (213 mg, 1.2 mmol) were added to a solution of **5a** (300 mg, 0.61 mmol) in a 1:1 mixture of chloroform/methanol (80 mL) at 0 °C and the reaction mixture was stirred for 1.5 h at that temperature. Chloroform (50 mL) was added and the solution was extracted twice with a saturated solution of Na_2SO_3 and washed with water. The organic phase was dried over Na_2SO_4 and evaporated to dryness. The brown residue was recrystallized from dichloromethane/methanol at −30 °C. The obtained solid was dried *in vacuo* to give 345 mg (0.46 mmol, 76%) of the desired dipyrrin as a dark blue powder. ^{1}H NMR (500 MHz, $CDCl_3$): δ = 14.88 (br s, 1H), 7.53 (d, J = 6.5 Hz, 4H), 7.39 (d, J = 16 Hz, 2H), 7.37−7.33 (m, 6H), 7.25 (d, J = 16 Hz, 2H), 6.97 (s, 2H), 2.37 (s, 3H), 2.11 (s, 6H), 1.41 (s, 6H); ^{13}C NMR (125 MHz, $CDCl_3$): δ = 149.75, 142.55, 138.62, 138.56, 137.46, 136.53, 135.68, 133.33, 133.22, 128.99, 128.79, 128.60, 127.45, 119.61, 85.95, 21.25, 19.79, 15.60; HR-ESI-TOF-MS (m/z): M^+, calculated for $C_{36}H_{32}I_2N_2^+$, 746.0655; found, 746.0605.

Synthesis of 5f. A solution of dipyrrin **6** (300 mg, 0.40 mmol), 4-ethynyltoluene (140 mg, 1.2 mmol), copper(I) iodide (3.8 mg, 0.020 mmol) and $Pd(PPh_3)_2Cl_2$ (14.1 mg, 0.020 mmol) in triethylamine (25 mL) was degassed and heated to 70 °C. The reaction mixture was stirred at room temperature overnight and evaporated to dryness *in vacuo* after addition of aluminum oxide. The residue was subjected to column chromatography on aluminum oxide (alumina, dichloromethane/hexane =1/4) and all blue fractions were collected and evaporated to dryness *in vacuo*. Recrystallization of the dark purple solid from dichloromethane/methanol at −30 °C and drying *in vacuo* yielded the pure product as a dark purple solid (200 mg, 69%). ^{1}H NMR (500 MHz, $CDCl_3$): δ = 14.55 (br s, 1H), 7.68 (d, J = 16 Hz, 2H), 7.60 (d, J = 7.4 Hz, 4H), 7.42 (t, J = 8.0 Hz, 4H), 7.40 (d, J = 7.6 Hz, 4H), 7.36 (d, J = 16 Hz, 2H), 7.34−7.32 (m, 2H), 7.17 (d, J = 7.8 Hz, 4H), 6.98 (s, 2H), 2.38 (s, 9H), 2.14 (s, 6H), 1.54 (s, 6H); ^{13}C NMR (125 MHz, $CDCl_3$): δ = 151.00, 142.62, 138.65, 138.41, 138.34, 138.08, 136.93, 135.70, 133.14, 132.38, 131.13, 129.15, 128.88, 128.82, 128.47, 127.24, 120.77, 118.98, 115.01, 97.21, 82.71, 21.50, 21.26, 19.72, 12.43; HR-ESI-TOF-MS (m/z): M^+, calculated for $C_{54}H_{46}N_2^+$, 722.3661; found, 722.3658.

Synthesis of 2,8-Diiodo-1,3,7,9-tetramethyl-5-(2,4,6-trimethylphenyl)dipyrrin (7). To a chloroform/methanol =1:1 solution (40 mL) of **4** (318 mg, 1.0 mmol) and iodine (510 mg, 2.0 mmol), an aqueous solution (5 mL) of iodic acid (352 mg, 2.0 mmol) was added and stirred 1 h at room temperature. The solution was diluted with chloroform (100 mL) and the organic layer was washed with an aqueous solution of sodium sulfite (5%) and potassium bicarbonate (1%). The organic layer was dried over sodium sulfate and evaporated to give the pure product as a red brown powder (506 mg, 89%). ^{1}H NMR (500 MHz, $CDCl_3$): δ = 13.81 (br s, 1H), 6.92 (s, 2H), 2.40 (s, 6H), 2.34 (s, 3H), 2.05 (s, 6H), 1.30 (s, 6H); ^{13}C NMR (125 MHz, $CDCl_3$): δ = 151.86, 141.40, 138.22, 137.72, 135.56, 135.50, 133.46, 128.84, 83.08, 21.21, 19.55, 17.09, 15.63; HR-ESI-TOF-MS (m/z): $[M + H]^+$, calculated for $C_{22}H_{25}I_2N_2^+$, 571.0107; found, 571.0009.

Synthesis of 1,9-Bis[(*E*)-2-(2,4-dimethoxyphenyl)ethenyl]-2,8-diiodo-3,7-dimethyl-5-(2,4,6-trimethylphenyl)dipyrrin (8). To a *N,N*-dimethylformamide solution (15 mL) of dipyrrin **7** (285 mg, 0.50 mmol) and 2,4-dimethoxybenzaldehyde (333 mg, 2.0 mmol), acetic acid (0.5 mL) and piperidine (0.5 mL) were added and the reaction mixture was heated to 90 °C for 6 h. After cooling the solution, the solution was diluted with ethyl acetate and washed with brine. The organic layer was dried over Na_2SO_4 and evaporated. The reaction mixture was processed by column chromatography (alumina, diethyl ether/hexane =1/4) followed by recrystallization from dichloromethane/methanol to give the pure product as a dark purple solid (92 mg, 21%). ^{1}H NMR (500 MHz, $CDCl_3$): δ = 14.96 (br s,

DOI: 10.1021/jacs.6b02128
J. Am. Chem. Soc. 2016, 138, 5666−5677

1H), 7.62 (d, J = 16 Hz, 2H), 7.56 (d, J = 8.5 Hz, 2H), 7.13 (d, J = 16 Hz, 2H), 6.95 (s, 2H), 6.47 (dd, J = 8.5, 2.2 Hz, 2H), 6.29 (d, J = 2.6 Hz, 2H), 3.84 (s, 6H), 3.28 (s, 6H), 2.36 (s, 3H), 2.10 (s, 6H), 1.39 (s, 6H); ^{13}C NMR (125 MHz, $CDCl_3$): δ = 161.19, 158.93, 150.34, 141.78, 138.24, 135.94, 135.88, 133.65, 128.86, 128.83, 128.03, 119.52, 117.34, 104.75, 97.87, 85.30, 55.47, 54.72, 21.25, 19.83, 15.49 (one carbon peak is missing because of overlaps with other peaks); HR-FAB-MS (m/z): M^+, calculated for $C_{40}H_{40}I_2N_2O_4^+$, 866.1077; found, 866.1096.

Synthesis of 5g. A solution of the dipyrrin **8** (100 mg, 0.12 mmol), 4-ethynyltoluene (55 mg, 0.47 mmol), copper(I) iodide (1.2 mg, 6.4 μmol) and $Pd(PPh_3)_2Cl_2$ (4.2 mg, 6.0 μmol) in triethylamine (10 mL) was degassed and heated to 70 °C. The reaction mixture was stirred at room temperature overnight and evaporated to dryness *in vacuo* after addition of aluminum oxide. The residue was subjected to column chromatography (alumina, dichloromethane/hexane =1/2) and all blue fractions were collected and evaporated to dryness *in vacuo*. Recrystallization from dichloromethane/methanol and drying *in vacuo* yielded the crude product **5g** as a dark purple solid (66 mg, 68%), which was used in the next reaction without purification.

Synthesis of 1,9-Bis[(*E*)-2-(2-thienyl)ethenyl]-2,8-diiodo-3,7-dimethyl-5-(2,4,6-trimethylphenyl)dipyrrin (9). Iodine (200 mg, 0.79 mmol) and iodic acid (139 mg, 0.79 mmol) were added to a solution of the dipyrrin **5c** (200 mg, 0.395 mmol) in a 1:1 mixture of chloroform/methanol (60 mL) at 0 °C and the reaction mixture was stirred for 1.5 h at that temperature. Chloroform (50 mL) was added and the solution was extracted twice with a saturated solution of Na_2SO_3 and washed with water. The organic phase was dried over Na_2SO_4 and evaporated to dryness. The brown residue was recrystallized from dichloromethane/methanol at −30 °C. The obtained solid was dried *in vacuo* to give the desired dipyrrin as a dark blue powder (171 mg, 57%). ^{1}H NMR (500 MHz, $CDCl_3$): δ = 14.73 (br s, 1H), 7.42 (d, J = 16 Hz, 2H), 7.33−7.32 (m, 2H), 7.06−7.05 (m, 4H), 7.04 (d, J = 16 Hz, 2H), 6.96 (s, 2H), 2.36 (s, 3H), 2.09 (s, 6H), 1.39 (s, 6H); ^{13}C NMR (125 MHz, $CDCl_3$): δ = 149.33, 142.56, 142.46, 138.75, 138.55, 136.86, 135.72, 133.30, 128.98, 128.38, 127.96, 126.15, 125.84, 119.06, 85.77, 21.25, 19.78, 15.62; HR-ESI-TOF-MS (m/z): M^+, calculated for $C_{32}H_{28}I_2N_2S_2^+$, 758.9783; found, 758.9747.

Synthesis of 5h. A solution of the dipyrrin **9** (250 mg, 0.33 mmol), 4-ethynyltoluene (115 mg, 0.99 mmol), copper(I) iodide (3.1 mg, 0.016 mmol) and $Pd(PPh_3)_2Cl_2$ (11.6 mg, 0.016 mmol) in triethylamine (20 mL) was degassed and heated to 70 °C. The reaction mixture was stirred at room temperature overnight and evaporated to dryness *in vacuo* after addition of aluminum oxide. The residue was subjected to column chromatography (alumina, dichloromethane/hexane = 1/3) and all blue fractions were collected and evaporated to dryness *in vacuo*. Recrystallization from dichloromethane/methanol at −30 °C and drying *in vacuo* yielded the desired product **5h** as a dark blue solid (165 mg, 68%). ^{1}H NMR (500 MHz, $CDCl_3$): δ = 14.43 (br s, 1H), 7.80 (d, J = 16 Hz, 2H), 7.41 (d, J = 8.0 Hz, 4H), 7.32 (d, J = 5.0 Hz, 2H), 7.17−7.16 (m, 6H), 7.14 (d, J = 16 Hz, 2H), 7.08 (dd, J = 5.0, 3.7 Hz, 2H), 6.97 (s, 2H), 2.37 (s, 9H), 2.12 (s, 6H, 1.51n(s, 6H); ^{13}C NMR (125 MHz, $CDCl_3$): δ = 150.50, 142.83, 142.57, 138.72, 138.32, 138.06, 137.88, 135.73, 133.12, 131.07, 129.16, 128.86, 127.99, 127.74, 126.03, 125.91, 120.76, 118.64, 114.71, 97.40, 82.80. 21.50, 21.25, 19.69, 12.40; HR-ESI-TOF-MS (m/z): M^+, calculated for $C_{50}H_{42}N_2S_2^+$, 734.2789; found, 734.2767.

Synthesis of 1a. To a dichloromethane solution (20 mL) of dipyrrin **4** (63.3 mg, 0.20 mmol) and π-expanded dipyrrin **5a** (48.7 mg, 0.10 mmol) was added zinc acetate (27.8 mg, 0.15 mmol). The solution was stirred for 3 h at room temperature and evaporated. The residue was filtered by Millipore and processed with GPC to isolate the crude product. Recrystallization from dichloromethane/methanol yielded the pure product as a brown solid (15.7 mg, 18%). ^{1}H NMR (500 MHz, $CDCl_3$): δ = 7.20−7.12 (m, 10H), 6.99 (d, J = 16 Hz, 2H), 6.96 (s, 2H), 6.88−6.85 (m, 4H), 6.59 (s, 2H), 5.96 (s, 2H), 2.37 (s, 3H), 2.32 (s, 3H), 2.14 (s, 6H), 2.10 (s, 6H), 1.90 (s, 6H), 1.37 (s, 12H); ^{13}C NMR (125 MHz, $CDCl_3$): δ = 156.52, 155.79, 143.67, 143.48, 137.94, 137.30, 135.96, 134.98, 132.24, 128.85, 128.67, 128.43, 127.47, 126.96, 122.29, 120.28, 117.28, 21.24, 21.20, 19.57, 16.48, 15.17, 14.88; HR-FAB-MS (m/z): M^+, calculated for $C_{58}H_{58}N_4Zn^+$, 874.3953; found, 874.3934.

Synthesis of 1b. To a dichloromethane solution (20 mL) of dipyrrin **4** (32.2 mg, 0.10 mmol) and π-expanded dipyrrin **5b** (61.7 mg, 0.10 mmol) was added zinc acetate (18.6 mg, 0.10 mmol). The solution was stirred for 3 h at room temperature and evaporated. The residue was filtered by Millipore and processed with GPC to isolate the crude product. Recrystallization from dichloromethane/hexane yielded the pure product as an ocher solid (23.2 mg, 23%). ^{1}H NMR (500 MHz, $CDCl_3$): δ = 7.32 (d, J = 16 Hz, 2H), 6.96−6.94 (m, 4H), 6.83 (s, 2H), 6.70 (d, J = 16 Hz, 2H), 6.60 (s, 2H), 6.36 (d, J = 2.6 Hz, 2H), 6.26 (dd, J = 8.5, 2.6 Hz, 2H), 5.94 (s, 2H), 3.79 (s, 6H), 3.77 (s, 6H), 2.36 (s, 3H), 2.31 (s, 3H), 2.14 (s, 6H), 2.09 (s, 6H), 1.88 (s, 6H), 1.36 (s, 6H), 1.35 (s, 6H); ^{13}C NMR (125 MHz, $CDCl_3$): δ = 160.55, 157.74, 156.50, 156.32, 143.80, 143.31, 142.89, 141.22, 137.47, 137.26, 136.41, 136.14, 136.03, 134.91, 128.71, 128.55, 127.36, 126.09, 120.44, 120.11, 119.89, 117.12, 105.44, 97.88, 55.50, 55.42, 21.23, 21.21, 19.57, 19.55, 16.44, 15.15, 14.88 (two quaternary carbons are missing because of overlaps with other peaks); HR-FAB-MS (m/z): $[M + H]^+$, calculated for $C_{62}H_{67}N_4O_4Zn^+$, 995.4453; found, 995.4468.

Synthesis of 1c. To a dichloromethane solution (20 mL) of dipyrrin **4** (31.2 mg, 0.10 mmol) and π-expanded dipyrrin **5c** (50.5 mg, 0.10 mmol) was added zinc acetate (18.2 mg, 0.10 mmol). The solution was stirred for 3 h at room temperature and evaporated. The residue was filtered by Millipore and processed with GPC to isolate the crude product. Recrystallization from dichloromethane/methanol yielded the pure product as an ocher solid (8.9 mg, 10%). ^{1}H NMR (500 MHz, $CDCl_3$): δ = 7.11−7.04 (m, 4H), 6.95 (s, 2H), 6.89−6.85 (m, 6H), 6.70 (d, J = 16 Hz, 2H), 6.52 (s, 2H), 5.96 (s, 2H), 2.36 (s, 3H), 2.32 (s, 3H), 2.13 (s, 6H), 2.10 (s, 6H), 1.96 (s, 6H), 1.35 (s, 12H); ^{13}C NMR (125 MHz, $CDCl_3$): δ = 156.37, 155.38, 144.05, 143.67, 143.42, 142.61, 142.12, 138.22, 137.74, 137.30, 136.12, 136.08, 136.01, 135.99, 135.13, 128.84, 128.60, 127.63, 125.39, 124.97, 124.68, 121.88, 120.28, 117.43, 21.23, 21.20, 19.65, 19.59, 16.50, 15.14, 14.95; HR-FAB-MS (m/z): $[M + H]^+$, calculated for $C_{54}H_{55}N_4S_2Zn^+$, 887.3160; found, 887.3184.

Synthesis of 1d. To a dichloromethane solution (20 mL) of dipyrrin **4** (21.5 mg, 0.068 mmol) and π-expanded dipyrrin **5d** (38.1 mg, 0.070 mmol) was added zinc acetate (12.9 mg, 0.070 mmol). The solution was stirred for 3 h at room temperature and evaporated. The residue was filtered by Millipore and processed with GPC to isolate the crude product. Recrystallization from dichloromethane/methanol yielded the pure product as an ocher solid (16.9 mg, 27%). ^{1}H NMR (500 MHz, $CDCl_3$): δ = 7.32−7.31 (m, 8H), 7.23−7.21 (m, 2H), 7.01 (s, 2H), 6.95 (s, 2H), 6.82−6.77 (m, 2H), 6.63−6.52 (m, 6H), 6.44 (d, J = 15 Hz, 2H), 5.92 (s, 2H), 2.40 (s, 3H), 2.38 (s, 6H), 2.36 (s, 3H), 2.13 (s, 6H), 2.00 (s, 6H), 1.37 (s, 6H), 1.35 (s, 6H); ^{13}C NMR (125 MHz, $CDCl_3$): δ = 156.32, 155.33, 143.26, 143.22, 143.13, 141.87, 138.14, 137.73, 137.57, 137.41, 136.36, 136.10, 135.93, 135.42, 134.32, 133.04, 132.67, 129.74, 128.90, 128.82, 128.60, 127.50, 126.49, 126.37, 120.17, 117.63, 21.25, 19.94, 19.44, 16.16, 15.16, 14.87 (one methyl carbon is missing because of overlaps with other peaks); HR-FAB-MS (m/z): M^+, calculated for $C_{62}H_{62}N_4Zn^+$, 926.4266; found, 926.4239.

Synthesis of 1e. To a dichloromethane solution (20 mL) of dipyrrin **4** (81.2 mg, 0.25 mmol) and crude π-expanded dipyrrin **5e** (171 mg, 0.26 mmol) was added zinc acetate (46.4 mg, 0.25 mmol). The solution was stirred overnight at room temperature and evaporated. The residue was filtered by Millipore and processed with GPC to isolate the crude product. Recrystallization from dichloromethane/methanol yielded the pure product as an ocher solid (26.9 mg, 5.2% over 2 steps). ^{1}H NMR (500 MHz, $CDCl_3$): δ = 7.29 (d, J = 8.5 Hz, 2H), 6.99 (s, 2H), 6.94 (s, 2H), 6.84−6.79 (m, 4H), 6.52−6.46 (m, 6H), 6.42 (s, 2H), 6.37 (d, J = 15 Hz, 2H), 5.90 (s, 2H), 3.84 (s, 6H), 3.81 (s, 6H), 2.38 (s, 3H), 2.36 (s, 9H), 2.13 (s, 6H), 2.00 (s, 6H), 1.35 (s, 6H), 1.34 (s, 6H); ^{13}C NMR (125 MHz, $CDCl_3$): δ = 160.58, 157.87, 156.32, 155.55, 143.08, 142.91, 142.88, 141.02, 137.89, 137.59, 137.42, 136.54, 136.31, 136.08, 135.61, 134.28, 133.85, 128.81, 128.75, 128.11, 127.48, 126.75, 124.93, 120.15, 119.75, 117.42, 105.12, 98.47, 55.54, 55.46, 21.28, 19.99, 19.48, 16.18, 15.17,

DOI: 10.1021/jacs.6b02128
J. Am. Chem. Soc. 2016, 138, 5666−5677

14.89 (one methyl carbon are missing because of overlaps with other peaks); HR-FAB-MS (m/z): M^+, calculated for $C_{66}H_{70}O_4N_4Zn^+$, 1046.4688; found, 1046.4669.

Synthesis of 1f. To a dichloromethane solution (20 mL) of dipyrrin **4** (31.6 mg, 0.10 mmol) and π-expanded dipyrrin **5f** (72.0 mg, 0.10 mmol) was added zinc acetate (18.6 mg, 0.10 mmol). The solution was stirred overnight at room temperature and evaporated. The residue was filtered by Millipore and processed with GPC to isolate the crude product. Recrystallization from dichloromethane/methanol yielded the pure product as an ocher solid (11.3 mg, 10%). ^{1}H NMR (500 MHz, $CDCl_3$): δ = 8.19 (d, J = 16 Hz, 2H), 7.36 (d, J = 7.9 Hz, 4H), 7.18−7.09 (m, 16H), 6.99 (s, 2H), 6.81 (s, 2H), 6.00 (s, 2H), 2.39 (s, 3H), 2.35 (s, 6H), 2.31 (s, 3H), 2.15 (s, 6H), 2.13 (s, 3H), 1.79 (s, 6H), 1.36 (s, 6H) (one methyl proton peak is missing because of overlap with water peak); ^{13}C NMR (125 MHz, $CDCl_3$): δ = 156.36, 155.63, 147.04, 144.24, 144.07, 143.76, 138.29, 137.87, 137.79, 137.50, 137.38, 135.92, 135.86, 135.70, 135.34, 134.99, 130.72, 129.19, 129.15, 128.63, 128.50, 127.85, 127.23, 121.76, 121.13, 120.37, 112.95, 97.70, 84.91, 21.48, 21.26, 21.18, 19.64, 19.41, 16.64, 14.97, 13.48 (one quaternary carbon is missing because of overlaps with other peaks); HR-FAB-MS (m/z): M^+, calculated for $C_{76}H_{70}N_4Zn^+$, 1102.4892; found, 1102.4905.

Synthesis of 1g. To a dichloromethane solution (15 mL) of dipyrrin **4** (22.1 mg, 0.069 mmol) and π-expanded dipyrrin **5g** (58.5 mg, 0.069 mmol) was added zinc acetate (13.1 mg, 0.071 mmol). The solution was stirred overnight at room temperature and evaporated. The residue was filtered by Millipore and processed with GPC to isolate the crude product. Recrystallization from dichloromethane/methanol yielded the pure product as a green solid (17.4 mg, 21%). ^{1}H NMR (500 MHz, $CDCl_3$): δ = 8.54 (d, J = 16 Hz, 2H), 7.41 (d, J = 8.2 Hz, 2H), 7.10 (d, J = 7.9 Hz, 4H), 7.00−6.96 (m, 4H), 6.86 (d, J = 8.5 Hz, 2H), 6.80 (s, 2H), 6.36 (d, J = 2.3 Hz, 2H), 6.24 (dd, J = 8.5, 2.2 Hz, 2H), 5.98 (s, 2H), 3.79 (s, 6H), 3.66 (s, 6H), 2.38 (s, 3H), 2.34 (s, 6H), 2.30 (s, 3H), 2.13 (s, 6H), 2.12 (s, 6H), 1.80 (s, 6H), 1.53 (s, 6H), 1.34 (s, 6H); ^{13}C NMR (125 MHz, $CDCl_3$): δ = 160.85, 158.14, 156.34, 156.18, 146.51, 143.97, 143.69, 142.34, 138.02, 137.45, 137.33, 137.23, 135.99, 135.93, 135.82, 134.90, 130.99, 129.05, 129.00, 128.84, 128.52, 127.39, 121.48, 120.20, 120.09, 119.79, 112.42, 105.48, 97.77, 97.53, 85.05, 55.41, 55.26, 21.47, 21.26, 21.19, 19.62, 19.47, 16.58, 14.96, 13.43 (one carbon is missing because of overlaps with other peaks); HR-ESI-TOF-MS (m/z): M^+, calculated for $C_{80}H_{78}N_4O_4Zn^+$, 1222.5315; found, 1222.5276.

Synthesis of 1h. To a dichloromethane solution (20 mL) of dipyrrin **4** (31.9 mg, 0.10 mmol) and π-expanded dipyrrin **5h** (73.0 mg, 0.10 mmol) was added zinc acetate (18.8 mg, 0.10 mmol). The solution was stirred for overnight at room temperature and evaporated. The residue was filtered by Millipore and processed with GPC to isolate the crude product. Recrystallization from dichloromethane/methanol yielded the pure product as a brown solid (7.8 mg, 7%). ^{1}H NMR (500 MHz, $CDCl_3$): δ = 8.25 (d, J = 16 Hz, 2H), 7.36−7.34 (m, 4H), 7.15−7.12 (m, 6H), 6.98 (s, 2H), 6.94−6.83 (m, 8H), 5.99 (s, 2H), 2.38 (s, 3H), 2.35 (s, 6H), 2.31 (s, 3H), 2.14 (s, 6H), 2.12 (s, 6H), 1.89 (s, 6H), 1.52 (s, 6H), 1.34 (s, 6H); ^{13}C NMR (125 MHz, $CDCl_3$): δ = 156.27, 155.26, 146.76, 144.19, 144.06, 143.29, 142.83, 138.29, 138.14, 137.80, 137.33, 136.09, 135.93, 135.81, 135.72, 135.20, 130.69, 129.17, 129.13, 128.61, 127.80, 127.72, 125.86, 125.60, 121.08, 121.06, 120.43, 113.19, 97.87, 84.86, 21.47, 21.25, 21.18, 19.65, 19.46, 16.65, 14.99, 13.48; HR-ESI-TOF-MS (m/z): M^+, calculated for $C_{72}H_{66}N_4S_2Zn^+$, 1114.4020; found, 1114.3997.

Synthesis of 2a. Symmetric complex **2a** was retrieved as a byproduct when dissymmetric complex **1a** was synthesized. Recrystallization from dichloromethane/methanol yielded the pure product as an ocher solid (12.2 mg, 24%). ^{1}H NMR (500 MHz, $CDCl_3$): δ = 7.22−7.12 (m, 20H), 6.99 (d, J = 16 Hz, 4H), 6.85 (m, 8H), 6.64 (s, 4H), 2.35 (s, 6H), 1.91 (s, 12H), 1.44 (s, 12H); ^{13}C NMR (125 MHz, $CDCl_3$): δ = 156.20, 143.77, 142.91, 138.13, 137.76, 137.40, 136.26, 135.75, 132.65, 128.76, 128.39, 127.47, 127.02, 122.36, 118.21, 21.24, 19.57, 15.29; HR-FAB-MS (m/z): M^+, calculated for $C_{72}H_{66}N_4Zn^+$, 1050.4579; found, 1050.4550.

Synthesis of 2b. To a dichloromethane solution (15 mL) of π-expanded dipyrrin **5b** (49.9 mg, 0.081 mmol) was added zinc acetate (7.5 mg, 0.041 mmol). The solution was stirred for overnight at room temperature and evaporated. Recrystallization from dichloromethane/hexane yielded the pure product as a red brown solid (32.8 mg, 62%). ^{1}H NMR (500 MHz, $CDCl_3$): δ = 7.28 (d, J = 16 Hz, 4H), 6.99 (d, J = 8.5 Hz, 4H), 6.84 (s, 4H), 6.73 (d, J = 16 Hz, 4H), 6.63 (s, 4H), 6.34 (d, J = 2.2 Hz, 4H), 6.26 (dd, J = 8.5, 2.2 Hz, 4H), 3.79 (s, 12H), 3.74 (s, 12H), 2.33 (s, 6H), 1.90 (s, 12H), 1.40 (s, 12H); ^{13}C NMR (125 MHz, $CDCl_3$): δ = 160.46, 157.76, 156.71, 142.88, 141.36, 137.62, 137.35, 136.52, 136.18, 128.49, 127.50, 126.31, 120.73, 120.10, 117.83, 105.37, 97.91, 55.50, 55.40, 21.23, 19.62, 15.26; HR-ESI-TOF-MS (m/z): M^+, calculated for $C_{80}H_{82}N_4O_8Zn^+$, 1290.5424; found, 1290.5481.

Synthesis of 2c. Symmetric complex **2c** was retrieved as a byproduct when dissymmetric complex **1c** was synthesized. Recrystallization from dichloromethane/methanol yielded the pure product as an ocher solid (7.8 mg, 7%). ^{1}H NMR (500 MHz, $CDCl_3$): δ = 7.10 (d, J = 4.9 Hz, 4H), 7.07 (d, J = 16 Hz, 4H), 6.88−6.86 (m, 8H), 6.84 (d, J = 3.4 Hz, 4H), 6.69 (d, J = 16 Hz, 4H), 6.58 (s, 4H), 2.34 (s, 6H), 1.95 (s, 12H), 1.41 (s, 12H); ^{13}C NMR (125 MHz, $CDCl_3$): δ = 155.61, 143.80, 142.82, 142.61, 138.54, 137.64, 136.42, 135.79, 128.68, 127.55, 125.59, 124.95, 124.93, 122.05, 118.37, 21.24, 19.54, 15.38; HR-ESI-TOF-MS (m/z): M^+, calculated for $C_{64}H_{58}N_4S_4Zn^+$, 1074.2836; found, 1074.2856.

Synthesis of 2d. Symmetric complex **2d** was retrieved as a byproduct when dissymmetric complex **1d** was synthesized. Recrystallization from dichloromethane/methanol yielded the pure product as a red brown solid (5.5 mg, 7%). ^{1}H NMR (500 MHz, $CDCl_3$): δ = 7.33−7.29 (m, 16H), 7.23−7.20 (m, 4H), 7.05 (s, 4H), 6.78 (dd, J = 15, 10 Hz, 12H), 6.39 (d, J = 15 Hz, 4H), 2.42 (s, 18H), 1.43 (s, 12H); ^{13}C NMR (125 MHz, $CDCl_3$): δ = 155.68, 143.09, 141.30, 137.95, 137.86, 137.42, 136.20, 135.76, 133.22, 133.07, 129.62, 128.98, 128.57, 127.50, 126.37, 126.24, 118.30, 21.29, 20.23, 15.24; HR-FAB-MS (m/z): M^+, calculated for $C_{80}H_{74}N_4Zn^+$, 1154.5205; found, 1154.5203.

Synthesis of 2e. To a dichloromethane solution (20 mL) of crude π-expanded dipyrrin **5e** (103 mg, 0.15 mmol) was added zinc acetate (27.3 mg, 0.15 mmol). The solution was stirred for overnight at room temperature and evaporated. The residue was filtered by Millipore and processed with GPC to isolate the crude product. Recrystallization from dichloromethane/hexane yielded the pure product as a red brown solid (23.1 mg, 11% over 2 steps). ^{1}H NMR (500 MHz, $CDCl_3$): δ = 7.29 (d, J = 8.5 Hz, 4H), 7.02 (s, 4H), 6.81−6.76 (m, 8H), 6.50−6.29 (m, 20H), 3.84 (s, 12H), 3.79 (s, 12H), 6.26 (dd, J = 8.5, 2.2 Hz, 4H), 3.79 (s, 12H), 3.74 (s, 12H), 2.41 (s, 6H), 2.40 (s, 12H), 1.40 (s, 12H); ^{13}C NMR (125 MHz, $CDCl_3$): δ = 160.50, 157.82, 155.84, 142.49, 140.34, 137.62, 137.55, 136.55, 136.04, 134.06, 128.78, 128.05, 127.39, 126.65, 124.83, 119.84, 118.05, 105.08, 98.42, 55.52, 55.42, 21.29, 20.28, 15.22; HR-ESI-TOF-MS (m/z): M^+, calculated for $C_{88}H_{90}N_4O_8Zn^+$, 1394.6050; found, 1394.6038.

Synthesis of 2f. Symmetric complex **2f** was retrieved as a byproduct when dissymmetric complex **1f** was synthesized. Recrystallization from dichloromethane/methanol yielded the pure product as a red solid (19 mg, 13%). ^{1}H NMR (500 MHz, $CDCl_3$): δ = 8.14 (d, J = 16 Hz, 4H), 7.34 (d, J = 7.8 Hz, 8H), 7.19−7.17 (m, 20H), 7.11 (d, J = 7.7 Hz, 8H), 6.96 (d, J = 16 Hz, 4H), 6.82 (s, 4H), 2.33 (s, 18H), 1.68 (s, 12H), 1.55 (s, 12H); ^{13}C NMR (125 MHz, $CDCl_3$): δ = 156.08, 147.27, 144.50, 138.19, 137.74, 137.52, 136.28, 136.05, 135.15, 132.38, 130.80, 129.11, 128.90, 128.55, 127.93, 127.26, 121.45, 121.11, 114.16, 97.73, 84.56, 21.45, 21.22, 19.22, 13.64; HR-ESI-TOF-MS (m/z): M^+, calculated for $C_{108}H_{90}N_4Zn^+$, 1506.6458; found, 1506.6406.

Synthesis of 2g. Symmetric complex **2g** was retrieved as a byproduct when dissymmetric complex **1g** was synthesized. Recrystallization from dichloromethane/methanol yielded the pure product as a purple solid (19.6 mg, 16%). ^{1}H NMR (500 MHz, $CDCl_3$): δ = 8.50 (d, J = 16 Hz, 4H), 7.38 (d, J = 8.2 Hz, 8H), 7.07 (d, J = 7.9 Hz, 8H), 6.98 (d, J = 8.5 Hz, 4H), 6.88 (d, J = 16 Hz, 4H), 6.83 (s, 4H), 6.34−6.30 (m, 8H), 3.77 (s, 12H), 3.65 (s, 12H), 2.33 (s, 6H), 2.32 (s, 12H), 1.76 (s, 12H), 1.53 (s, 12H); ^{13}C NMR (125 MHz, $CDCl_3$): δ = 160.86, 158.28, 156.62, 146.56, 142.65, 137.86, 137.68, 137.22,

DOI: 10.1021/jacs.6b02128
J. Am. Chem. Soc. 2016, 138, 5666−5677

136.49, 135.61, 131.00, 128.80, 128.68, 127.69, 121.62, 120.37, 119.82, 113.38, 105.48, 97.96, 97.45, 85.12, 55.40, 55.31, 21.43, 21.23, 19.34, 13.58; HR-ESI-TOF-MS (m/z): M^+, calculated for $C_{116}H_{106}N_4O_8Zn^+$, 1746.7302; found, 1746.7288.

Synthesis of 2h. Symmetric complex **2h** was retrieved as a byproduct when dissymmetric complex **1h** was synthesized. Recrystallization from dichloromethane/methanol yielded the pure product as a red purple solid (11.0 mg, 7%). ^{1}H NMR (500 MHz, $CDCl_3$): δ = 8.14 (d, J = 16 Hz, 4H), 7.33 (d, J = 7.9 Hz, 8H), 7.15 (d, J = 4.7 Hz, 4H), 7.11 (d, J = 7.8 Hz, 8H), 6.90 (t, J = 4.3 Hz, 6H), 6.86−6.85 (m, 6H), 6.78 (d, J = 16 Hz, 4H), 2.34 (s, 6H), 2.33 (s, 12H), 1.79 (s, 12H), 1.55 (s, 12H); ^{13}C NMR (125 MHz, $CDCl_3$): δ = 155.66, 147.04, 142.95, 138.67, 138.24, 137.71, 136.52, 130.78, 129.09, 128.90, 128.29, 127.77, 126.46, 125.76, 121.12, 120.86, 114.44, 97.81, 84.64, 73.67, 59.86, 21.45, 21.24, 19.24, 13.75; HR-ESI-TOF-MS (m/z): M^+, calculated for $C_{100}H_{82}N_4S_4Zn^+$, 1530.4714; found, 1530.4568.

■ ASSOCIATED CONTENT

Supporting Information

The Supporting Information is available free of charge on the ACS Publications website at DOI: 10.1021/jacs.6b02128.

Previous examples of dissymmetric bis(dipyrrinato)zinc(II) and tris(dipyrrinato)indium(III) complexes; synthetic procedures for π-expanded dipyrrins **5a−h**; comparisons of ^{1}H NMR spectra among corresponding dissymmetric and symmetric complexes; crystallographic data of complexes **1e·CH$_2$Cl$_2$** and **2a·CH$_3$OH**; UV/vis spectra of symmetric complexes **2a−h** and **3** in toluene; frontier orbital ordering of **1a−e** and **1h**; examples of π-expanded BODIPYs, including Figures S1−S13, Scheme S1, and Tables S1 and S2 (PDF)

X-ray crystallographic file for **1e·CH$_2$Cl$_2$** (CIF)

X-ray crystallographic file for **2a·CH$_3$OH** (CIF)

■ AUTHOR INFORMATION

Corresponding Authors

*sakamoto@chem.s.u-tokyo.ac.jp

*nisihara@chem.s.u-tokyo.ac.jp

Notes

The authors declare no competing financial interest.

■ ACKNOWLEDGMENTS

The present article was supported by Grants-in-Aid from MEXT of Japan (Nos. 26620039, 26220801, 26708005, 15H00862, 16H00900, 16H00957, areas 2406 [All Nippon Artificial Photosynthesis Project for Living Earth], 2506 [Science of Atomic Layers], and 2509 [Molecular Architectonics]). R.S. is grateful to Asahi Glass Foundation, Iketani Science and Technology Foundation, The MIKIYA Science and Technology Foundation, Yazaki Memorial Foundation for Science and Technology, Shorai Foundation for Science and Technology, The Hitachi Global Foundation, Kumagai Foundation for Science and Technology, Foundation for Interaction in Science & Technology (FIST), The Foundation Advanced Technology Institute, Izumi Science and Technology Foundation, The Foundation for The Promotion of Ion Engineering, LIXIL JS Foundation, Tonen General Sekiyu R&D Encouragement and Assistance Foundation, and the IWATANI NAOJI foundation for financial supports. M.T. thanks JSPS Research Fellowship for young scientists, and Advanced Leading Graduate Course for Photon Science (ALPS). J.F.K. acknowledges JSPS Postdoctoral Fellowship for Overseas Researchers.

■ REFERENCES

(1) (a) Loudet, A.; Burgess, K. *Chem. Rev.* **2007**, *107*, 4891−4932. (b) Wood, T. E.; Thompson, A. *Chem. Rev.* **2007**, *107*, 1831−1861. (c) Ulrich, G.; Ziessel, R.; Harriman, A. *Angew. Chem., Int. Ed.* **2008**, *47*, 1184−1202.

(2) (a) Baker, J. G.; Adams, L. A.; Salchow, K.; Mistry, S. N.; Middleton, R. J.; Hill, S. J.; Kellam, B. *J. Med. Chem.* **2011**, *54*, 6874−6887. (b) Kobayashi, T.; Komatsu, T.; Kamiya, M.; Campos, C.; González-Gaitán, M.; Terai, T.; Hanaoka, K.; Nagano, T.; Urano, Y. *J. Am. Chem. Soc.* **2012**, *134*, 11153−11160. (c) Ni, Y.; Wu, J. *Org. Biomol. Chem.* **2014**, *12*, 3774−3791.

(3) (a) Shah, M.; Thangaraj, K.; Soong, M. L.; Wolford, L.; Boyer, J. H.; Politzer, I. R.; Pavlopoulos, T. G. *Heteroat. Chem.* **1990**, *1*, 389−399. (b) Lai, R. Y.; Bard, a J. *J. Phys. Chem. B* **2003**, *107*, 5036−5042. (c) Bañuelos, J.; Martín, V.; Gómez-Durán, C. F. A.; Córdoba, I. J. A.; Peña-Cabrera, E.; García-Moreno, I.; Costela, Á.; Pérez-Ojeda, M. E.; Arbeloa, T.; Arbeloa, Í. L. *Chem. - Eur. J.* **2011**, *17*, 7261−7270.

(4) Sakamoto, R.; Iwashima, T.; Tsuchiya, M.; Toyoda, R.; Matsuoka, R.; Kögel, J. F.; Kusaka, S.; Hoshiko, K.; Yagi, T.; Nagayama, T.; Nishihara, H. *J. Mater. Chem. A* **2015**, *3*, 15357−15371.

(5) (a) Yu, L.; Muthukumaran, K.; Sazanovich, I. V.; Kirmaier, C.; Hindin, E.; Diers, J. R.; Boyle, P. D.; Bocian, D. F.; Holten, D.; Lindsey, J. S. *Inorg. Chem.* **2003**, *42*, 6629−6647. (b) Ma, L.; Patrick, B. O.; Dolphin, D. *Chem. Commun.* **2011**, *47*, 704−706. (c) Zhang, Y.; Thompson, A.; Rettig, S. J.; Dolphin, D. *J. Am. Chem. Soc.* **1998**, *120*, 13537−13538. (d) Maeda, H.; Nishimura, T.; Akuta, R.; Takaishi, K.; Uchiyama, M.; Muranaka, A. *Chem. Sci.* **2013**, *4*, 1204−1211.

(6) (a) Maeda, H.; Hasegawa, M.; Hashimoto, T.; Kakimoto, T.; Nishio, S.; Nakanishi, T. *J. Am. Chem. Soc.* **2006**, *128*, 10024−10025. (b) Sakamoto, R.; Hoshiko, K.; Liu, Q.; Yagi, T.; Nagayama, T.; Kusaka, S.; Tsuchiya, M.; Kitagawa, Y.; Wong, W.-Y.; Nishihara, H. *Nat. Commun.* **2015**, *6*, 6713. (c) Matsuoka, R.; Toyoda, R.; Sakamoto, R.; Tsuchiya, M.; Hoshiko, K.; Nonoguchi, Y.; Nishibori, E.; Kawai, T.; Nishihara, H. *Chem. Sci.* **2015**, *6*, 2853−2858. (d) Do, L.; Halper, S. R.; Cohen, S. M. *Chem. Commun.* **2004**, *23*, 2662−2663.

(7) (a) Halper, S. R.; Do, L.; Stork, J. R.; Cohen, S. M. *J. Am. Chem. Soc.* **2006**, *128*, 15255−15268. (b) Béziau, A.; Baudron, S. A.; Fluck, A.; Hosseini, M. W. *Inorg. Chem.* **2013**, *52*, 14439−14448. (c) Béziau, A.; Baudron, S. A.; Guenet, A.; Hosseini, M. W. *Chem. - Eur. J.* **2013**, *19*, 3215−3223. (d) Béziau, A.; Baudron, S. A.; Rogez, G.; Hosseini, M. W. *Inorg. Chem.* **2015**, *54*, 2032−2039.

(8) Baudron, S. A. *Dalton Trans.* **2013**, *42*, 7498−7509.

(9) Sazanovich, I. V.; Kirmaier, C.; Hindin, E.; Yu, L.; Bocian, D. F.; Lindsey, J. S.; Holten, D. *J. Am. Chem. Soc.* **2004**, *126*, 2664−2665.

(10) Trinh, C.; Kirlikovali, K.; Das, S.; Ener, M. E.; Gray, H. B.; Djurovich, P.; Bradforth, S. E.; Thompson, M. E. *J. Phys. Chem. C* **2014**, *118*, 21834−21845.

(11) Filatov, M. A.; Lebedev, A. Y.; Mukhin, S. N.; Vinogradov, S. A.; Cheprakov, A. V. *J. Am. Chem. Soc.* **2010**, *132*, 9552−9554.

(12) (a) Kusaka, S.; Sakamoto, R.; Kitagawa, Y.; Okumura, M.; Nishihara, H. *Chem. - Asian J.* **2012**, *7*, 907−910. (b) Kusaka, S.; Sakamoto, R.; Nishihara, H. *Inorg. Chem.* **2014**, *53*, 3275−3277.

(13) (a) Halper, S. R.; Stork, J. R.; Cohen, S. M. *Dalton Trans.* **2007**, 1067−1074. (b) Szymańska, I.; Stobiecka, M.; Orlewska, C.; Rohand, T.; Janssen, D.; Dehaen, W.; Radecka, H. *Langmuir* **2008**, *24*, 11239−11245. (c) Grabowska, I.; Maes, W.; Ngo, T. H.; Rohand, T.; Dehaen, W.; Radecki, J.; Radecka, H. *Int. J. Electrochem. Sci.* **2014**, *9*, 1232−1249. (d) Miao, Q.; Shin, J.-Y.; Patrick, B. O.; Dolphin, D. *Chem. Commun.* **2009**, 2541−2543.

(14) (a) Zhao, Y.; Zhang, Y.; Lv, X.; Liu, Y.; Chen, M.; Wang, P.; Liu, J.; Guo, W. *J. Mater. Chem.* **2011**, *21*, 13168−13171. (b) Guliyev, R.; Coskun, A.; Akkaya, E. U. *J. Am. Chem. Soc.* **2009**, *131*, 9007−9013. (c) Qu, X.; Liu, Q.; Ji, X.; Chen, H.; Zhou, Z.; Shen, Z. *Chem. Commun.* **2012**, *48*, 4600−4602. (d) Han, J.; Engler, A.; Qi, J.; Tung, C. H. *Tetrahedron Lett.* **2013**, *54*, 502−505.

DOI: 10.1021/jacs.6b02128
J. Am. Chem. Soc. 2016, 138, 5666−5677

(15) (a) Jenekhe, S. A.; Osaheni, J. A. *Science* **1994**, *265*, 765. (b) Hsieh, B. R.; Yu, Y.; Forsythe, E. W.; Schaaf, G. M.; Feld, W. A. *J. Am. Chem. Soc.* **1998**, *120*, 231. (c) Peng, Z.; Zhang, J.; Xu, B. *Macromolecules* **1999**, *32*, 5162. (d) Mikroyannidis, J. A. *Macromolecules* **2002**, *35*, 9289−9295.
(16) Suresh, D.; Lopes, P. S.; Ferreira, B.; Figueira, C. A.; Gomes, C. S. B.; Gomes, P. T.; Di Paolo, R. E.; Maçanita, A. L.; Duarte, M. T.; Charas, A.; Morgado, J.; Calhorda, M. J. *Chem. - Eur. J.* **2014**, *20*, 4126−4140.
(17) (a) Rohand, T.; Qin, W.; Boens, N.; Dehaen, W. *Eur. J. Org. Chem.* **2006**, *20*, 4658−4663. (b) Tsuchiya, M.; Sakamoto, R.; Kusaka, S.; Kitagawa, Y.; Okumura, M.; Nishihara, H. *Chem. Commun.* **2014**, *50*, 5881−5883.
(18) Kögel, J. F.; Kusaka, S.; Sakamoto, R.; Iwashima, T.; Tsuchiya, M.; Toyoda, R.; Matsuoka, R.; Tsukamoto, T.; Yuasa, J.; Kitagawa, Y.; Kawai, T.; Nishihara, H. *Angew. Chem., Int. Ed.* **2016**, *55*, 1377−1381.
(19) Toyoda, R.; Tsuchiya, M.; Sakamoto, R.; Matsuoka, R.; Wu, K.-H.; Hattori, Y.; Nishihara, H. *Dalton Trans.* **2015**, *44*, 15103−15106.
(20) Evans, D. H. *Chem. Rev.* **2008**, *108*, 2113−2144.
(21) Aguirre-Etcheverry, P.; O'Hare, D. *Chem. Rev.* **2010**, *110*, 4839−4864.
(22) Pommerehne, J.; Vestweber, H.; Guss, W.; Mahrt, R. F.; Bassler, H.; Porsch, M.; Daub, J. *Adv. Mater.* **1995**, *7*, 551−554.
(23) (a) Chen, J.; Burghart, A.; Derecskei-Kovacs, A.; Burgess, K. *J. Org. Chem.* **2000**, *65*, 2900−2906. (b) Dost, Z.; Atilgan, S.; Akkaya, E. U. *Tetrahedron* **2006**, *62*, 8484−8488. (c) Hayashi, Y.; Obata, N.; Tamaru, M.; Yamaguchi, S.; Matsuo, Y.; Saeki, A.; Seki, S.; Kureishi, Y.; Saito, S.; Yamaguchi, S.; Shinokubo, H. *Org. Lett.* **2012**, *14*, 866−869. (d) Umezawa, K.; Nakamura, Y.; Makino, H.; Citterio, D.; Suzuki, K. *J. Am. Chem. Soc.* **2008**, *130*, 1550−1551.
(24) Meyers, A. I.; Tomioka, K.; Fleming, M. P. *J. Org. Chem.* **1978**, *43*, 3788−3789.

DOI: 10.1021/jacs.6b02128
J. Am. Chem. Soc. 2016, 138, 5666−5677